REPUBLIC OF TURKEY
ACIBADEM MEHMET ALİ AYDINLAR UNIVERSITY
INSTITUTE OF HEALTH SCIENCES

MODIFICATION OF CATALYTIC SUBUNIT OF DNA POLYMERASE GAMMA BY CRISPR/CAS9 GENOME EDITING TECHNOLOGY

AYŞEGÜL EKMEKÇİOĞLU

MASTER THESIS

DEPARTMENT of MEDICAL BIOTECHNOLOGY

SUPERVISOR
Prof. Dr. Meltem MÜFTÜOĞLU

SECOND SUPERVISOR
Dr. Emre DENİZ

ISTANBUL - 2018

REPUBLIC OF TURKEY
ACIBADEM MEHMET ALİ AYDINLAR UNIVERSITY
INSTITUTE OF HEALTH SCIENCES

MODIFICATION OF CATALYTIC SUBUNIT OF DNA POLYMERASE GAMMA BY CRISPR/CAS9 GENOME EDITING TECHNOLOGY

AYŞEGÜL EKMEKÇİOĞLU

MASTER THESIS

DEPARTMENT of MEDICAL BIOTECHNOLOGY

SUPERVISOR
Prof. Dr. Meltem MÜFTÜOĞLU

SECOND SUPERVISOR
Dr. Emre DENİZ

ISTANBUL - 2018

Program:	Medical Biotechnology
Thesis title:	Modification Of Catalytic Subunit Of DNA Polymerase Gamma By Crispr/Cas9 Genome Editing Technology
Students' name and surname:	Ayşegül Ekmekçioğlu
Date of defence:	06 / 07 / 2018

This is to certify that I have examined this copy of master thesis. I have found that she prepared after fulfilling requirements specified in the associated legislations before the final examining committee whose signatures are below.

Jury president	Prof. Dr. Tanıl KOCAGÖZ Acıbadem Mehmet Ali Aydınlar University	Sign
Supervisor of the thesis	Prof. Dr. Meltem MÜFTÜOĞLU Acıbadem Mehmet Ali Aydınlar University	Sign
Second Supervisor of the thesis	Dr. Emre DENİZ Acıbadem Mehmet Ali Aydınlar University	Sign
Jury member	Prof. Dr. Tanıl KOCAGÖZ Acıbadem Mehmet Ali Aydınlar University	Sign
Jury member	Prof. Dr. Uğur SEZERMAN Acıbadem Mehmet Ali Aydınlar University	Sign
Jury member	Prof. Dr. Batu ERMAN Sabancı University	

This thesis has been approved by the above jury and it has been accepted by decision of Health Sciences Board of Directors.

Sign

Prof. Dr. Uğur ÖZBEK

Director of the Institute

Acıbadem Mehmet Ali Aydınlar University

DECLARATION

I hereby declare that, this thesis has been written by me based on the data obtained in line with the scientific rules and ethical principles of responsible conduct of research. All information, data, comments, analyses have been collected and processed through scientific, academic writing style, and literature used have been duly shown by giving reference to the original sources in accordance with the publication ethics. I also announce and emphasize that I have not violated any rules secured by patent and copyrights whilst the conduct and writing of this research.

06.07.2018

AYŞEGÜL EKMEKÇİOĞLU

ACKNOWLEDGEMENT

As a masters degree student, I wish to express my appreciation and gratitude to my university, my reputable advisors, my beloved colleagues-friends and my dear family. First and foremost, I thank my supervisor Prof. Dr. Meltem Müftüoğlu for not only her help for my thesis but also accepting me as her student 2 years ago. Her supreme guidance provided me and my fellow friends golden opportunities. Also, I appreciate her for making me and my fellow friends to participate in Genome Maintenance, DNA Repair and Cancer Meeting and introduce us too many reputable world-known scientists. I am deeply grateful for her belief and her worthwhile and supportive efforts. I would also express my gratitude to my second supervisor Dr. Emre Deniz for his patience to all my endless questions.

This study was supported by the Scientific and Technological Research Council of Turkey (TUBITAK), grant no:215S614. I would like to thank TUBITAK for its support. Furthermore, I am very thankful to Acıbadem Mehmet Ali Aydınlar University for providing us the world standard laboratories.

Many of my fellow friends have had encouraged me not to give up and supported me by providing helpful critiques. Over and above, I feel very lucky to have precious friends. First of all, I graciously thank Gülin Baran for her infinite assistance in laboratory works especially during bacterial culture experiments. I have always felt her support and persistent help through this journey. Moreover, I am grateful to have Ece Aksoy who brings joy to my life and she is my endorsement on technical issues by helping my unending requests. She is a wonderful friend that makes my life easier with her spiritual supports. Finally, I appreciate having Gizem Şele as one of my best friend for being there during tough times and cheering me up with her witty humor.

Lastly, I would like to thank my mother Özlenen Ekmekçioğlu, my father Melih Ekmekçioğlu and my sincere sister Zeynep Ekmekçioğlu for their support and patience during these challenging times. I also appreciate their understanding about my both physical and emotional absences. I am blessed to have my family's infinite love and unconditional support. They always wanted me to pursue my dreams as a scientist and supported me on every aspect of my education. Without them I would not be able to accomplish this journey.

TABLE OF CONTENTS

LIST OF ABBREVIATIONS

8-oxoG	8-oxoguanine
Acetyl CoA	Acetyl Coenzyme A
ADP	Adenosine diphosphate
AID	Accessory interacting domain
ANT	Adenine nucleotide translocase
amp	Ampicillin
AP site	Apurinic/apyrimidic site
APE1	AP Endonuclease 1
APS	Ammonium persulfate
ATP	Adenosine triphosphate
BER	Base excision repair
BSA	Bovine serum albumin
bp	Base pairs
Cas9	CRISPR-associated protein 9
Cas protein	CRISPR-associated protein
Col	Colony
CRISPR	Clustered regularly interspaced short palindromic repeats
crRNA	CRISPR RNA
ddH_2O	Double distilled water
DNA	Deoxyribonucleic acid
DNA2	DNA replication helicas/nuclease 2
dNTP	Deoxyribonucleotide triphosphate
dRP	Deoxyribose phosphate
DSB	Double strand break
dsDNA	Double-stranded DNA
DTT	1,4-Dithiothreitol
E.coli	*Escherichia coli*
ETC	Electron Transport Chain
EDTA	Ethylenediaminetetraacetid acid
EXOG	Exonuclease G
$FADH_2$	Flavin adenine dinucleotide
FEN1	Flap endonuclease 1
fwd	Forward
G6P	Glucose-6-phosphate
GFP	Green fluorescent protein
gRNA	Guide RNA
GTP	Guanosine triphosphate
H_2O	Water
H_2O_2	Hydrogen peroxide
HCT116	Human colorectal carcinoma 116 cell line

HCT116_Chr3	HCT116 Chromosome 3 cell line
HDR	Homology-directed repair
HK	Hexokinase
IP domain	Intrinsic processivity domain
IPTG	Isopropylv beta-D-1-thiogalactopyranoside
kb	Kilobase
kDa	Kilodalton
LB	Laemmli buffer
LIG3	DNA ligase III
LP-BER	Long-patch base excision repair
Mg^{2+}	Magnesium ion
MitoVES	Mitochondrially targeted vitamin E succinate
µL	Microliters
mL	Mililiters
MLH1	MutL homolog 1
MLS	Mitochondrial localization signals
MMR	Mismatch repair
MPP^{+}	1-methyl-4-phenylpyridinium
mtBER	Mitochondrial BER
mtDNA	Mitochondrial DNA
MTS	Mitochondrial targeting sequences
mtSSP	Mitochondrial single-stranded protein
NaCl	Sodium chloride
$NADH_2$	Nicotinamide adenine dinucleotide
NaF	Sodium fluoride
Na_3VO_4	Sodium orthovanadate
nBER	Nuclear BER
ND1	NADH dehydrogenase subunit 1
ND2	NADH dehydrogenase subunit 2
ND3	NADH dehydrogenase subunit 3
ND4	NADH dehydrogenase subunit 4
ND4L	NADH dehydrogenase subunit 4L
ND5	NADH dehydrogenase subunit 5
ND6	NADH dehydrogenase subunit 6
NHEJ	Non-homologous end-joining
nm	Nanometer
O_2	Oxygen
O_2^-	Superoxide anion
oligo	Oligodeoxynucleotide
OH^-	Hydroxyl radical
OXPHOS	Oxidative phosphorylation

PAM	Protospacer adjacent motif
PCR	Polymerase chain reaction
PEI	Polyethylenimine
PL	Partitioning loop
PMSF	Phenylmethylsulphonyl fluoride
PNK	Polynucleotide Kinase
polβ	Polymerase beta
polγ	Polymerase gamma
POLG	DNA polymerase gamma gene
POLG2	DNA polymerase gamma 2 gene
Puro	pSpCas9(BB)-2A-Puro
RFLP	Restriction Fragment Length Polymorphism
RITOLS	RNA incorporated throughout the lagging strand
RNA	Ribonucleic acid
ROS	Reactive oxygen species
SDS	Sodium dodecyl sulfate
SOD	Superoxide dismutase
SP-BER	Short-patch base excision repair
SSB	Single-strand break
ssDNA	Single-stranded DNA
TALENs	Transcription activator-like effector nucleases
TCA	Tricarboxylic acid cycle
TE buffer	Tris-EDTA buffer
TEMED	Tetramethylethylendiamine
tracrRNA, trRNA	Trans-activating crRNA
VDAC	Voltage-dependent anion channel
vit K3	Vitamin K3
wt	Wild-type
ZFNs	Zinc-finger nucleases
X-gal	5-Bromo-4-chloro-3-indolyl-beta-D-galatopyranoside

LIST OF FIGURES

LIST OF TABLES

SUMMARY

The synthetic lethality between DNA polymerase γ (polγ) and MLH1 is an important approach to kill MLH1 mutated/deficient cancer cells selectively through the small molecule inhibitors of polγ. Polγ involves in mitochondrial base excision repair (BER) and tumor suppressor protein MLH1 plays a role in mismatch repair (MMR). Besides its repair function during DNA replication, MMR also involves in the repair of oxidative DNA damage where the major repair pathway is BER. The polγ inhibition is a powerful target for the selective cancer treatment. To determine if polγ inhibitors-mediated tumor or cancer cell death is only through the cellular function of polγ without affecting other cellular processes, polγ knockdown cells are needed. Therefore, the aim of this study was to create inhibited/mutated polγ protein in MLH1 deficient HCT116 colon cancer and MLH1 proficient HCT116_Chr3 cell lines by using CRISPR/Cas9 gene editing technology for polγ. The first exon of the catalytic subunit of polγ was targeted for the *polγ* gene silencing, because it has all the enzymatic activities. A frame-shift mutation was created on *polγ* gene by CRISPR/Cas9 technology which caused to the premature stop codon and then *polγ* gene silencing. Consequently, three of the single cell colonies were identified as polγ knockdown cells.

Keywords: Base excision repair, cancer, CRISPR/Cas9 technology, polγ, synthetic lethality

ÖZET

DNA Polimeraz Gama Katalitik Alt Ünitesi Gen Bölgesinin CRISPR/Cas9 Genom Düzenleme Teknolojisi ile Modifikasyonu

DNA polymerase γ (polγ) ve MLH1 arasındaki sentetik lethal ilişki, MLH1 mutasyonuna sahip/hasarlı kanser hücrelerinin polγ'nın küçük molekül inhibitörleri ile seçici olarak öldürülmesini sağlayabileceği için önemli bir yaklaşımdır. Polγ, mitokondriyel baz eksizyon tamir (BER) yolağında, tümör baskılayıcı protein MLH1 ise yanlış eşleme tamir (MMR) yolağında görev almaktadır. MMR, DNA replikasyonu sırasındaki tamir fonksiyonun yanı sıra temel tamir yolağı BER olan oksidatif DNA hasarının da tamirin de görev almaktadır. Seçici kanser tedavisi için polγ inhibisyonu önemli bir hedeftir. Polγ inhibitörleri aracılığıyla oluşan kanser hücrelerinin ölümlerinin diğer hücresel faaliyetleri etkilemeden sadece polγ'nın hücredeki fonksiyonuna bağlı olarak mı gerçekleştiğini belirlemek için polγ proteini susturulmuş hücrelere ihtiyaç duyulmaktadır. Bu nedenle, bu çalışma kapsamında *MLH1* geni mutasyonu taşıyan (HCT116) ve mutasyona uğramamış *MLH1* geni taşıyan (HCT116_Chr3) hücre hatlarında CRISPR/Cas9 genom düzenleme teknolojisi kullanılarak inhibe edilmiş/mutasyona uğratılmış polγ proteini elde edilmesi amaçlanmıştır. *Polγ* geninin susturulmasında, polγ proteinin enzimatik aktiviteye sahip olan katalitik alt ünitesinin birinci ekzonu hedeflenmiştir. Polγ proteininde CRISPR/Cas9 teknoloji kullanılarak erken stop kodonu yaratılarak gen susturulmuştur. Sonuç olarak, tekli hücre kolonilerinin üçünde *polγ* geni susturulmuştur.

Anahtar Kelimeler: BER, CRISPR/Cas9 teknolojisi, kanser, polγ, sentetik letalite

1. AIM OF STUDY

The synthetic lethality between DNA polymerase γ (polγ) and MLH1 is an important approach to kill MLH1 mutated/deficient cancer cells selectively through the small molecule inhibitors of polγ. MLH1 plays a role in mismatch repair (MMR) pathway. It is known that mutated *MLH1* gene cause defective MMR which causes nonpolyposis colon cancer (Lynch syndrome). Because MLH1 is a tumor suppressor protein, one allele of *MLH1* is present in normal cells. Polγ is involved in both mitochondrial base excision repair (BER) and mtDNA replication. The mitochondria are a good target for anticancer therapy because of the synthetic lethal approach and because the cancer cell mitochondria are different from the mitochondria in normal cells. To understand if polγ inhibitors-mediated tumor or cancer cell death is only through the cellular function of polγ without affecting other cellular processes, polγ knockdown cells are needed. In this thesis study, to determine the specificity of polγ inhibitor in *MLH1* mutated HCT116 colon cancer cells, we generated mutations in polγ protein by using CRISPR/Cas9 technology.

The research done in this thesis explains how polγ protein is silenced by using CRISPR/Cas9 technology. Polγ is a trimeric protein which has the catalytic subunit (polγA) and two accessory subunits (polγB). PolγA has polymerase, exonuclease and dRP lyase activities. PolγB has no intrinsic enzymatic activity but it enhances the catalytic activity of polγA subunit [26, 27]. Therefore, in this study, the polγA subunit was targeted using CRISPR/Cas9 technology. Targeted design aims to create a frameshift mutation by insertion-deletion (indel) mutations at the first exon of polγ. Consequently, a premature stop codon was expected due to the frameshift mutation. Thereby, the polγ protein loses its functionality due to an early stop codon and created mutations. Furthermore, the effect of silenced polγ will be examined in the HCT116 (MLH1-deficient) and HCT116_Chr3 (MLH1-proficient) cell lines.

2. INTRODUCTION

2.1. Mitochondria

Mitochondrion is one of the most important organelle found in almost every eukaryotic cell. From cell to cell the amount of mitochondria varies, and there is a correlation between the number of mitochondria and the metabolic activity of the cell [1].

2.1.1. Structure

The structure of mitochondrion is composed of two membranes called as inner membrane and outer membrane. It includes intermembrane space, matrix, and cristae [2]. The general illustration of a mitochondrion is shown in Figure 2.1. The outer membrane has smooth structure whereas inner membrane has infoldings called as cristae so that inner membrane has increased surface area. The intermembrane space is the part exists between the outer and the inner membranes. The other part is trapped inside the inner membrane and called as matrix [1].

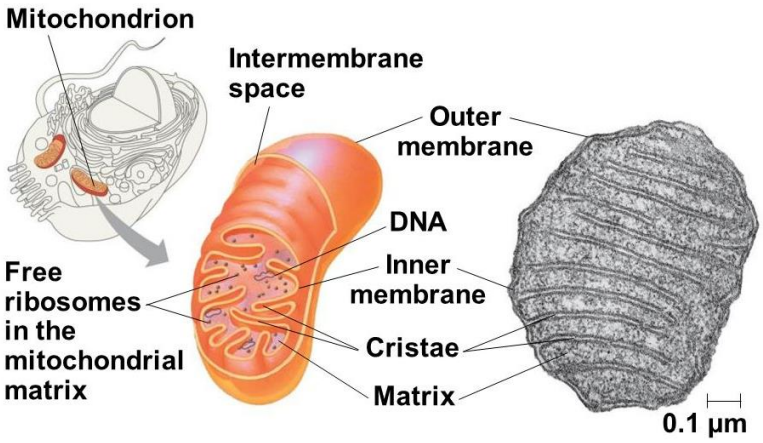

Figure 2.1. Illustrated image and electron micrograph of a mitochondrion. [1]

2.1.2. Function

Every part of mitochondrion has its unique function. Diffusion of molecules from outer membrane through the inner membrane is provided by the porins located on the outer membrane. Proteins that play a role in energetics and apoptosis are found in the intermembrane space. Transporters responsible for carrying proteins through the matrix and enzymes used for electron transport chain (ETC) are found mostly on the inner

membrane of mitochondria. The matrix includes the enzymes involved in the citric acid cycle [2]. Mitochondrion itself plays an important role as a powerhouse of a cell. Thus, the main source of adenosine triphosphate (ATP) is mitochondria. Generation of ATP is provided by mitochondrial ATP synthase from adenosine diphosphate (ADP) and phosphate ions which are the products of ATP hydrolysis. Mitochondria are involved in three main metabolic stages of cellular respiration which are glycolysis, citric acid cycle, and ETC and oxidative phosphorylation (OXPHOS) as shown in Figure 2.2. [1, 3]

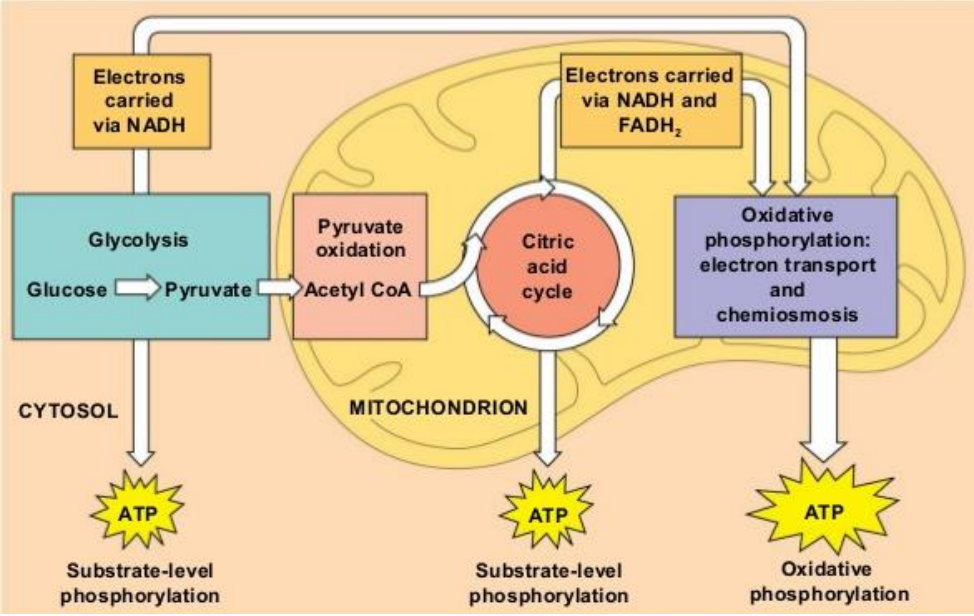

Figure 2.2. Summary of the cellular respiration. [1]

Glycolysis (first stage of respiration) occurs at cytosol and glucose is degraded into two pyruvate molecules. Then, second stage comes into play and in mitochondria pyruvate oxidized into a compound called acetyl Coenzyme A (acetyl CoA) which oxidized through citric acid cycle (TCA). Guanosine triphosphate (GTP), carbon dioxide, two flavin adenine dinucleotide ($FADH_2$), and two nicotinamide adenine dinucleotide ($NADH_2$) are products of TCA. Last and the third stage of the cellular respiration is OXPHOS [1]. In this step, ATP synthesis is generated by coupling of ETC to chemiosmosis as shown in Figure 2.3. Electrons are transferred through ETC complexes (Complex I–IV) by electron carriers produced at TCA, glycolysis etc. There are four ETC complexes responsible for electron transfer. Complex I is known as NADH dehydrogenase and plays a role in the oxidation of NADH. Then, oxidation of

$FADH_2$ is done by Complex II, succinate dehydrogenase. Coenzyme Q takes the electrons produced by Complex I-II and gives to Complex III (cytochrome reductase) and complex IV (cytochrome oxidase). Then, two protons (H^+) combined with oxygen and H_2O is produced. Through these electron transfer processes free energy is released into the mitochondrial inner membrane and an electrochemical gradient is formed. Then, ATP synthase uses this electrochemical gradient to produce ATP from ADP and this process is known as chemiosmosis. Thus, OXPHOS is made up from the combination of ETC and chemiosmosis [4].

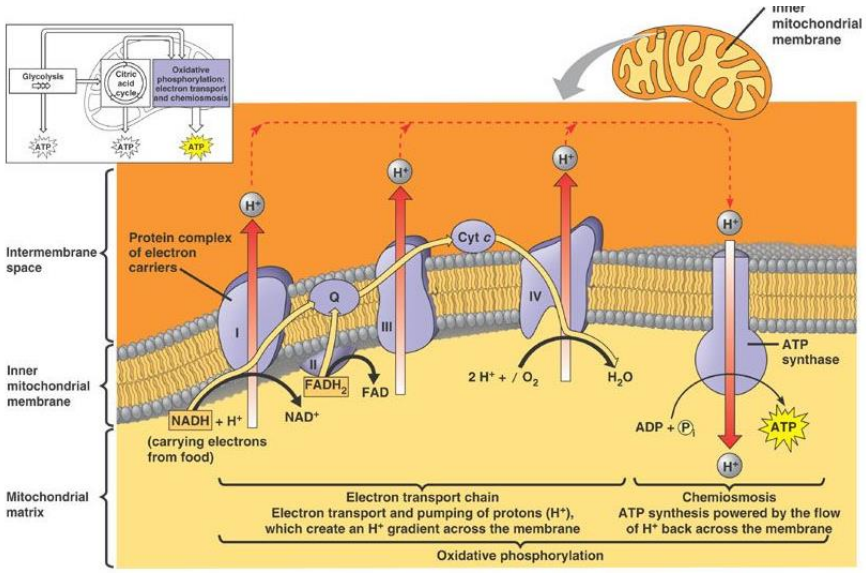

Figure 2.3. Electron transport chain and Oxidative phosphorylation. [1]

Mitochondria are also involved in the production of reactive oxygen species (ROS). ROS production is important for mitochondria since it could disrupt the redox signaling, causing mitochondrial dysfunction ending up with apoptosis [5]. Three forms of ROS exist which are known as superoxide anions (O_2^-), hydrogen peroxide (H_2O_2) and hydroxyl radicals (OH^-). As shown in Figure 2.4, when one electron is reduced from the molecular oxygen, ROS is produced. The unpaired electron of O_2^- reacts with superoxide dismutase (SOD) and reduces to H_2O_2. Then, by the help of cellular antioxidants, H_2O_2 is reduced to H_2O and O_2 [6].

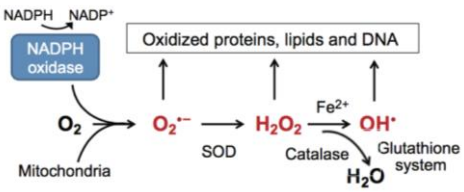

Figure 2.4. ROS Production. [6]

The main source of endogenous ROS production is ETC. In the normal flow, the reactions occur at ETC, oxygen is the final electron acceptor. However, somehow oxygen could be reduced through complex I and complex III which leads to the production of O_2^- as shown in Figure 2.5.

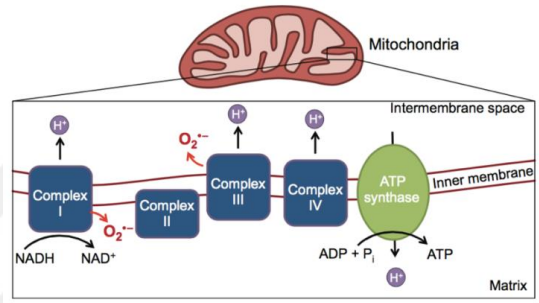

Figure 2.5. Redox reactions of the electron transport chain complexes. [6]

Mitochondria also play an important role in apoptosis which is known as programmed cell death. Apoptosis is divided into two pathways as an extrinsic and intrinsic pathway. The extrinsic pathway of apoptosis is regulated by membrane receptors whereas the intrinsic pathway is regulated by mitochondria [7]. The intrinsic apoptotic pathway is triggered by ROS (oxidative stress) and mitochondrial DNA (mtDNA) damage. As a result of this stimulation, the outer membrane of the mitochondrion becomes permeable due to the interaction between Bcl-2 family proteins and outer mitochondrial membrane. Bcl-2 protein family members are divided into two as anti-apoptotic (Bcl-2, Bcl-X_L, Bcl-w) and pro-apoptotic (Bax, Bad, Bak, Bim, Bid). Due to the cellular stress Bid is triggered and binds to Bax and Bax undergoes conformational change. Then, Bax is oligomerized to 6-8 molecules and cytochrome c is released from mitochondrion. In cytosol, cytochrome c and procaspase 9 are joined to form Apaf-1 and apoptosome is formed. Caspase 9 activates caspase 3 which cause DNA fragmentation and cell death [8].

The intrinsic pathway of apoptosis is summarized in Figure 2.6. On the other hand, Smac(second mitochondria-derived activator)/DIABLO, IAPs and NFκB (a transcription factor of inflammation) are the inhibitors of apoptosis proteins [7].

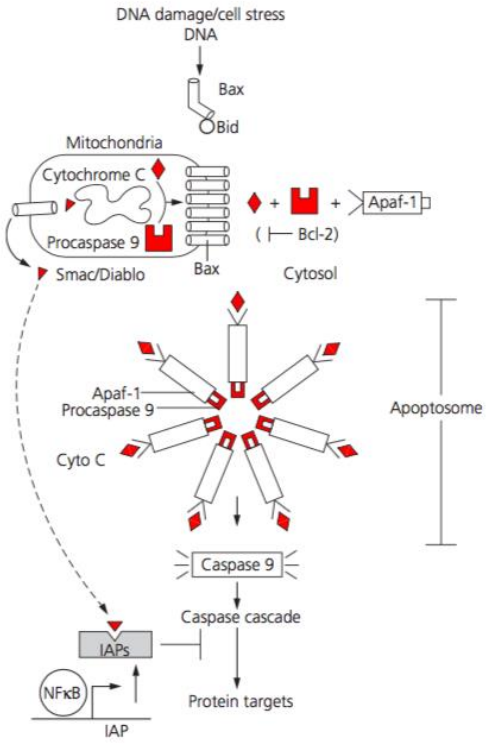

Figure 2.6. The intrinsic pathway of apoptosis. [7]

2.2. Mitochondrial DNA

Mitochondria have their own genome known as mtDNA. The location of mtDNA is in the matrix of mitochondrion and there exist several copies of mtDNA per mitochondrion [9].

2.2.1. Structure

MtDNA is composed of multiplies of circular double stranded DNA molecule with a size of 16.569 kb in humans. The structure of mtDNA is illustrated in Figure 2.7.

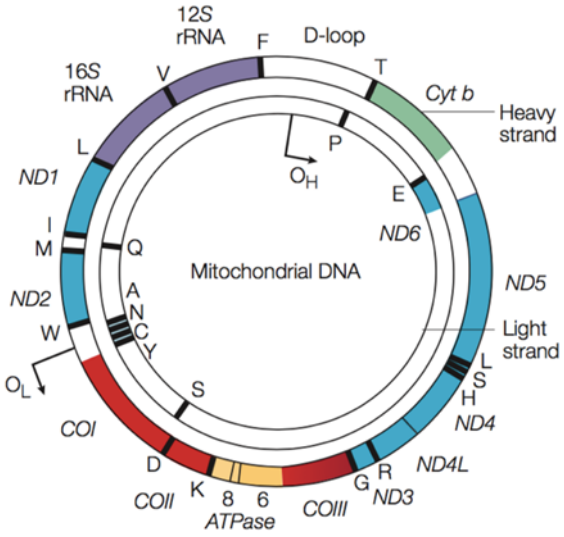

Figure 2.7. Human mitochondrial DNA. [10]

One of the strands of mtDNA is heavy (because it is guanine-rich strand) while the other one is light. Thirteen essential polypeptides used for OXPHOS system and RNA machinery are encoded by mtDNA. The subunits used for OXPHOS system are NADH dehydrogenase subunit 1-6 (ND1-6) and NADH dehydrogenase subunit 4L (ND4L) are for Complex I (blue); COI-COII are for cytochrome c oxidase (red); cytochrome b for Complex III (green) and finally ATPase 6 and 8 are for ATP synthase (yellow). The mtDNA also contains two ribosomal RNAs (purple; 12S and 16S) and 22 transfer RNAs (shown by black lines; single letter code denotation for protein synthesis). D-loop is the abbreviated form of displacement loop which indicates the non-coding control region of the mtDNA and includes the sequences needed for replication and transcription [10].

2.2.2. MtDNA replication

In an animal cell there are three ways to duplicate their genome which are strand-displacement, RITOLS and strand-coupled as illustrated in Figure 2.8. There are at least two separate origins of replication which can be named as origin of replication found on the heavy strand (O_H) for leading strand synthesis and origin of replication found on the light strand for lagging strand synthesis. In all models, replication of heavy strand is controlled by D-loop. In the strand-displacement model, new O_H starts to form in D-loop. As synthesis of O_H continues, replication of the light strand begins. In this model replication occurs continuously and asymmetrically and it is unidirectional.

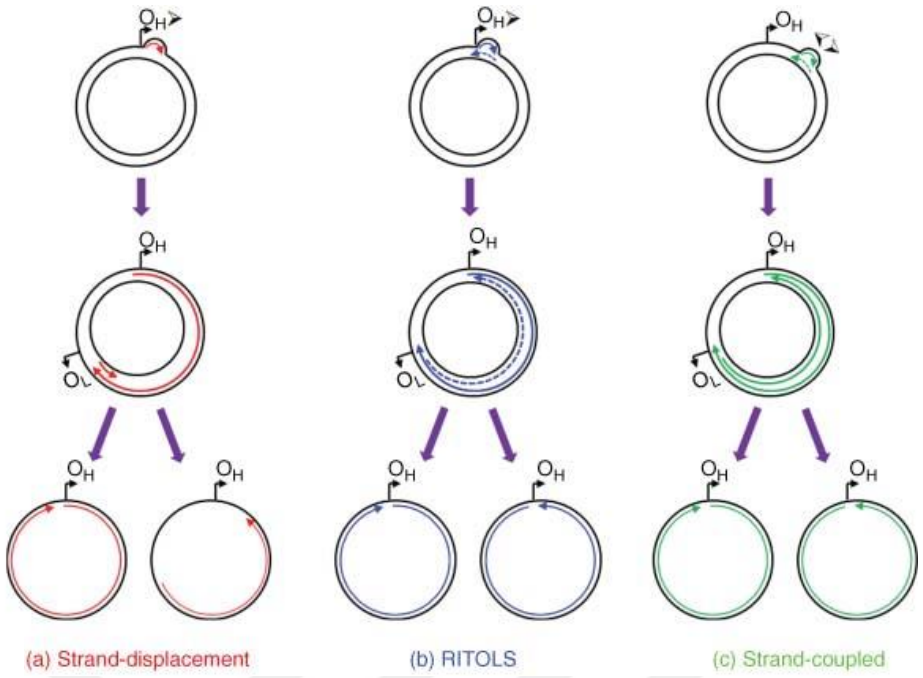

Figure 2.8. Mechanisms of mtDNA replication; **(a)** Strand-displacement, **(b)** RITOLS, **(c)** Strand-coupled. [12]

In strand-coupled model, replication is bidirectional [11]. In this model, replication begins with replication of heavy strand (O_H) combined with synthesis of light strand (O_L) [13]. The exact mechanism RITOLS model which is the abbreviated form of RNA incorporated throughout the lagging strand [12] is not known. However it is believed that RNA is produced complementary to the single-stranded DNA coming from the mtDNA transcription [14]. Replication of mtDNA is maintained by several proteins; Twinkle, polymerase gamma (polγ), and mitochondrial single-stranded protein [10]. Twinkle is a replicative helicase found on one of the DNA strand through 5'→3' direction that plays role in unwinding of dsDNA into ssDNA. Then, polγ uses the ssDNA provided by Twinkle as a template and maintains the DNA synthesis. Mitochondrial single-stranded protein is bound to ssDNA and prevents it from nucleolysis [11].

2.3. DNA Polymerase Gamma

In 1959, Arthur Kornberg discovered DNA polymerase in *Escherichia coli* (*E.coli*) [15]. Approximately 16 DNA polymerases are found in mammalian cells and each play role in different biological mechanism such as DNA replication (polymerases α, δ, ε, γ), DNA repair pathways (polymerase β, γ, λ, μ, θ), and genome maintenance (polymerases η, ι, κ, ζ) [16].

2.3.1. Structure

Polγ is a protein encoded by genes *POLG* (DNA polymerase gamma, catalytic subunit) and *POLG2* (DNA polymerase gamma 2, accessory subunit) which are located at long arm (q) of chromosome 15 and 17 respectively as shown in Figure 2.9 [17,18,19].

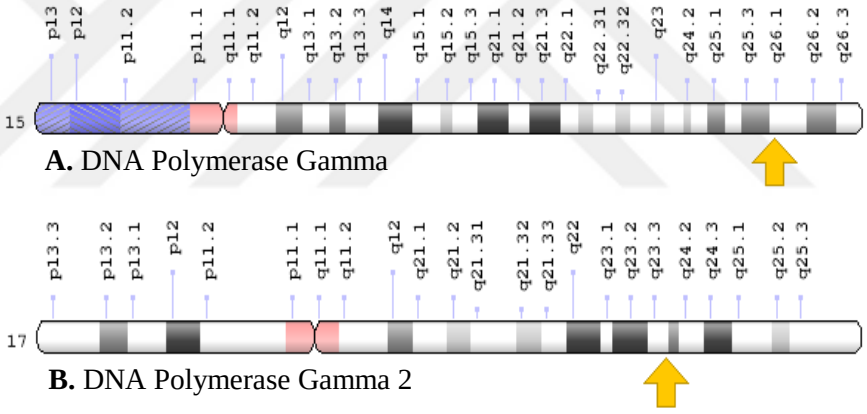

Figure 2.9. Chromosomal location of polγ. [18,19]

The basic structure of polγ is composed of three main subunits named as heterotrimeric catalytic subunit (polγA) and two accessory subunits (polγB) as shown in Figure 2.10 [20]. The catalytic subunit polγA is 140 kDa whereas the accessory subunit is 55 kDa [21].

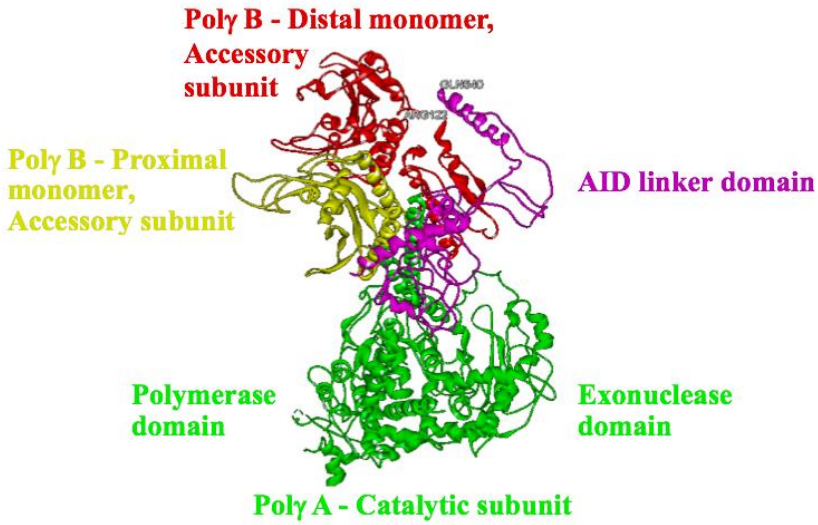

Figure 2.10. 3D-Structure of Polγ (Visualized by Discovery Studio, PDB ID:3IKM)

Mitochondrial proteins pass through the membrane of mitochondria by the help of direction of mitochondrial targeting sequences (MTS) or mitochondrial localization signals (MLS). Those signals are recognized by complexes called as TOM and TIM23. As shown in Figure 2.11, signal sequence of the precursor protein binds to TOM complex found on the outer mitochondrial membrane. Then, translocation of protein through the matrix is provided by the TIM23 complex attached to the inner mitochondrial membrane [22,23].

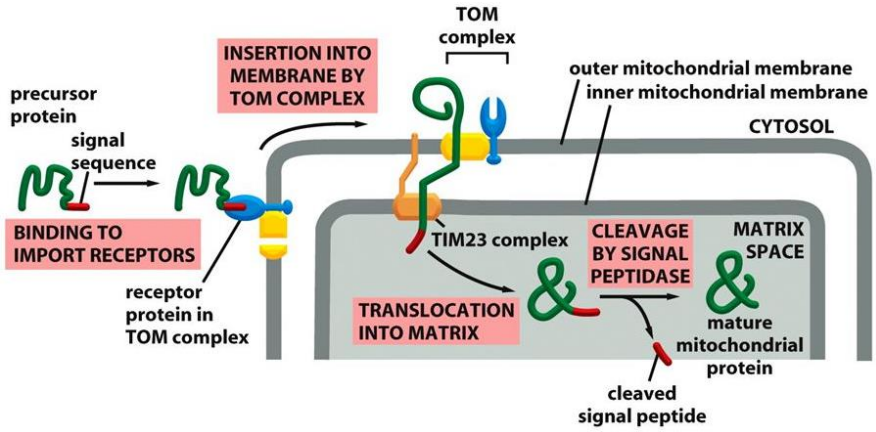

Figure 2.11. Importing proteins through mitochondria. [23]

As shown in Figure 2.12, polγ has MLS at its N-terminus. Moreover, it is separated into three major parts known as exonuclease domain (at N-terminus), spacer domain, and polymerase domain (C-terminus). Exonuclease domain owns the exo active site whereas polymerase domain has pol active site. Spacer domain provides separation between exonuclease and polymerase domain. It is divided into two parts as the

accessory interacting domain (AID) and intrinsic processivity (IP) domain. As name implies AID connects to the accessory subunit hydrophobically and provides DNA binding channel when the accessory subunit gets stabilized. IP domain also provides DNA binding channel however, it does not have connection with the accessory subunit. Polymerase domain has its own four subdomains: the thumb, the palm, partitioning loop, and the fingers. The connection between exonuclease-spacer domain and polymerase-spacer domain is provided by thumbs. Also, thumbs generate the major surface of DNA binding channel. Palm subdomain is the conserved structural module with catalytic part that plays role in coordination of two Mg^{2+} ions. The final subdomain of polymerase domain is fingers and it provides the binding of incoming dNTP substrate. PL is a stable structure that inserted into the fingers domain and provides the consistency of polγ [24].

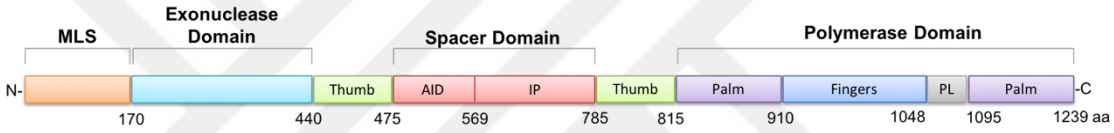

Figure 2.12. The catalytic subunit of polγ. [25]

2.3.2. Function

The catalytic subunit of polγ provides 3'→ 5' exonuclease activity and it binds to the accessory subunit by the help of amino acids found in the thumb subdomain. The accessory subunit increases the processing of polγ by providing a tight binding with DNA [26, 27]. The replication of mtDNA is provided by a set of proteins and polγ is one of them. Therefore, polγ plays an important role in mtDNA replication. Polγ was the only known replicative polymerase in the mitochondria until Bohr and colleagues demonstrated that polymerase beta (polβ) is also a mitochondrial polymerase [28, 29]. Unfortunately, mitochondria are vulnerable organelles since they are the major organelles for production of ROS by ETC. Thus, in order to protect the integrity of mtDNA maintenance, mitochondria need to have DNA repair system. Base excision repair (BER) is one of the main types of repair mechanism that is involved in mitochondria and it protects DNA from oxidized, alkylated, deaminated DNA lesions and abasic sites [30]. It is known that BER can either play a role in mitochondria and nucleus. The BER pathway can be divided into two sub-pathways known as long-patch

(LP) BER and short-patch (SP) BER. The mechanisms used for both nucleus or mitochondria are similar. However, mitochondrial BER (mtBER) proceeds an independent mechanism from the nuclear BER (nBER). According to recent studies, SP-BER was the repair mechanism used in mitochondria but now it is believed that mitochondria also have LP-BER As shown in Figure 2.13, BER is maintained by four main steps:

i. recognition of damaged DNA and removal of modified nucleotide by DNA glycosylases (an abasic site forms),
ii. cleavage of DNA backbone and formation of 3'-deoxyribose phosphate (dRP) site,
iii. gap formed is filled by polymerase activity of polγ,
iv. sealing of resultant nick by DNA ligase [31].

Since BER plays role both in mitochondria and nucleus, it is a crucial repair mechanism for the maintenance of the genomic stability. The main steps of BER pathway is described above. DNA glycosylases remove the modified base and an apurinic/apyrimidic site (AP site) is formed. DNA glycosylases can be mono- or bifunctional according to the sub-pathway where they enter. Monofunctional DNA glycosylases are used for LP-BER whereas bifunctional ones are for SP-BER. Then, AP sites are recognized by AP Endonuclease 1 (APE1) and a single-strand break (SSB) is created with a dRP region on the strand (flap) and the gap is filled by polγ. After this step, BER pathway could either go through SP-BER or LP-BER.

In SP-BER, polγ synthesizes a single nucleotide into the gap. On the other hand, in LP-BER two to thirteen nucleotides added to the gap using one or two polymerases (polβ or polγ/ε) and the flap formed is removed by the help of flap endonuclease 1 (FEN1), exonuclease G (EXOG), and DNA replication helicase/nuclease 2 (DNA2). Final step of BER is the ligation step and it is common for both sub-pathways. In the ligation step, the nick observed is sealed by DNA ligase III (LIG3) [32].

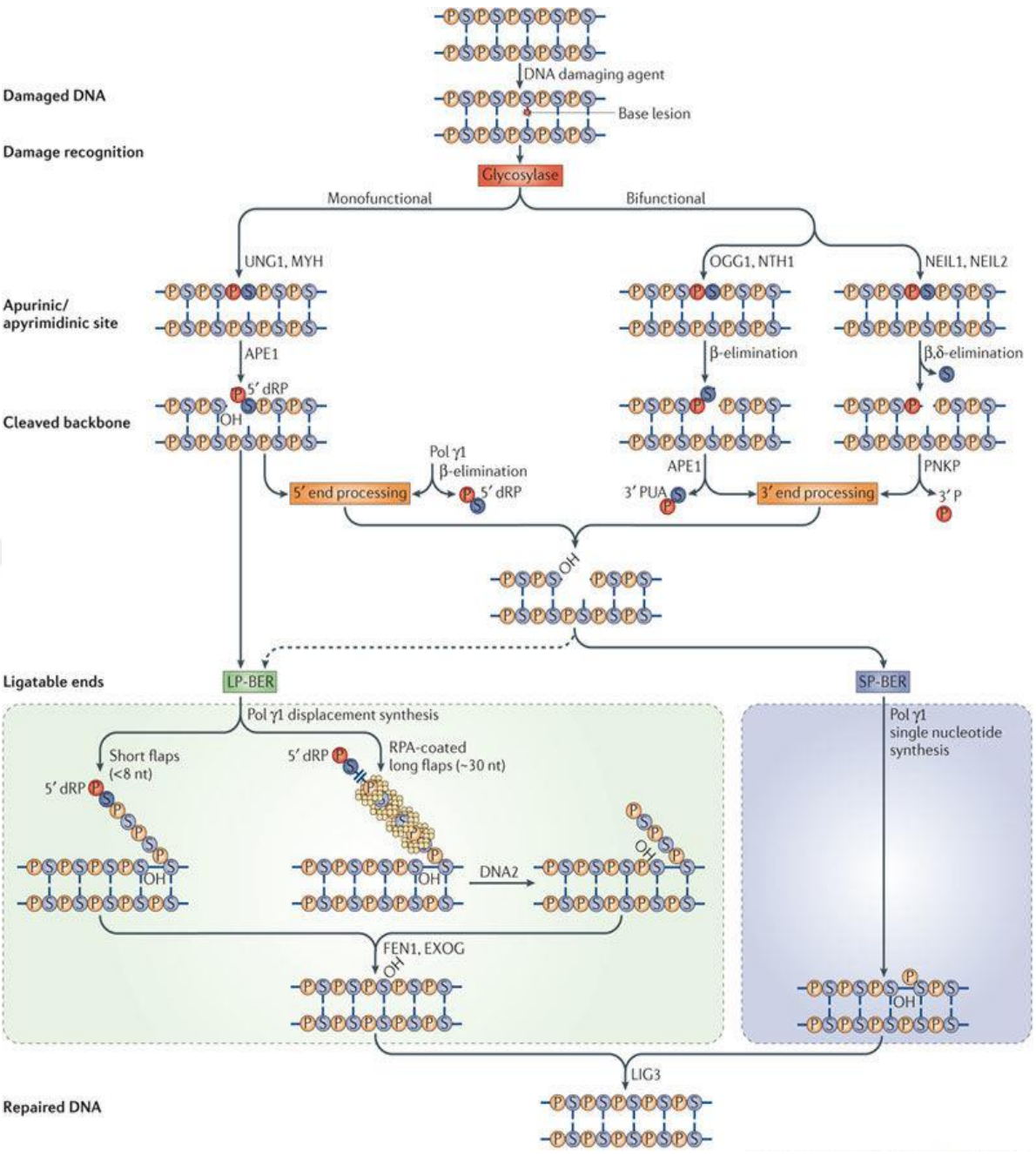

Figure 2.13. The base excision repair pathways. The capital letters of S and P represents the sugar-phosphate backbone of a DNA strand. UNG1, uracil-DNA glycosylase; MYH, MutY homologue; OGG1, 8-oxoguanine-DNA glycosylase 1; NTH1, endonuclease III; NEIL1, Endonuclease VIII-like 1; NEIL2, endonuclease VIII-like 2; APE1, apurinic/apyrimidinic endonuclease 1; PNKP, Polynucleotide kinase/phosphatase; 3'PUA, 3'-phospho-a-b-unsaturated aldehyde; 5'dRP, 5' deoxyribosephosphate; FEN1, flap endonuclease 1; EXOG, exonuclease G; DNA2, DNA replication helicase/nuclease 2, and LIG3, DNA ligase 3. [30]

2.3.3. Polγ in health and disease

The occurrence of mutations in mtDNA can affect the maintenance and the stability of mtDNA. The mutations can cause mitochondrial diseases. Mutations may occur due to the exogenous (e.g. smoking) or the endogenous sources (e.g. oxidative stress). In addition to all sources of mutations, spontaneous errors can also affect the maintenance of mtDNA due to defective mtDNA replication or repair. Most of the spontaneous errors can be caused by polγ. That's why proper functioning of polγ is very crucial for keeping mtDNA stable [33]. Over 300 point mutations linked to mitochondrial diseases. They could be either hereditary or based on mitochondrial dysfunction [22].

2.4. Targeting Mitochondria for Anti-cancer Therapy

In 1930s, Otto Warburg discovered that mitochondria of cancer cells were dysfunctional and ATP was produced through glycolysis. This phenomenon is known as Warburg Effect [34,35]. Later, it was shown that mitochondria are not dysfunctional in all cancer types but all of them have very active glycolytic pathway compared to normal cells. Thus, cancer cells consume higher amounts of glucose compared to normal cells. That's why the metabolism of mitochondria of cancer cells differs from the metabolism of normal cells as shown in Figure 2.14.

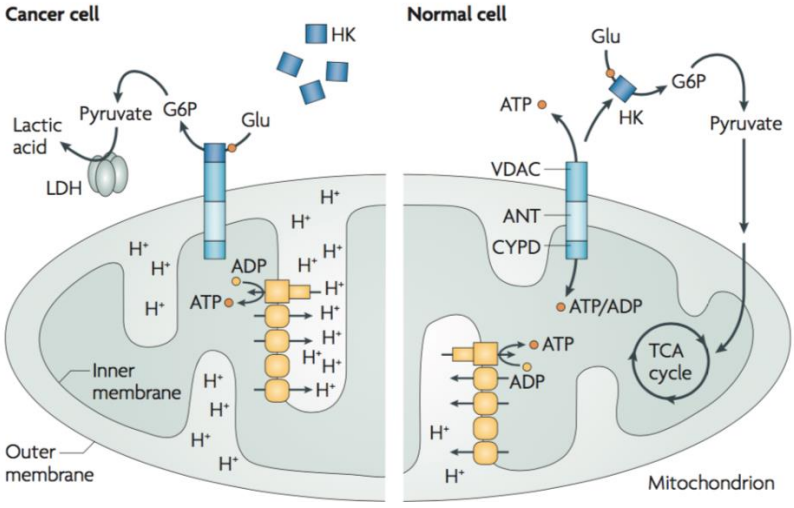

Figure 2.14. The mitochondrial metabolism of cancer cell versus normal cell. [36]

Because of the difference between the mitochondria in cancer cell and in normal cell, targeting mitochondria might be helpful for selective anti-cancer therapy. The term "mitocans" is used for agents that are used for the induction of apoptosis by

destabilizing mitochondria where “mito” stands for mitochondria and “cans” for cancer. Due to the molecular target, there are eight classes of mitocans as shown in Figure 2.15. The mitochondrial outer membrane is targeted by Class 1 agents. Class 1 agents inhibit the enzyme hexokinases (HK) [36]. HK is a glycolytic enzyme that phosphorylates glucose and turns it into glucose-6-phosphate (G6P). However, in cancer cells HK tightly binds to voltage-dependent anion channel (VDAC) and prevents the transportation of mitochondrial metabolites. Thus, inhibition of VDAC results with cancer cell growth [37]. Class 2 agents comprise small molecules that contain mimetic BH3 which inhibits family of Bcl-2 proteins. Agents that belong to Class 3 and Class 4 provide the inhibition of VDAC and adenine nucleotide translocase (ANT) proteins. The ETC and TCA are targeted by Class 5 and Class 7 agents respectively. Class 6 targets the mitochondrial inner membrane. The final class is the Class 8 and agents of this class are responsible for the maintenance of mtDNA [36].

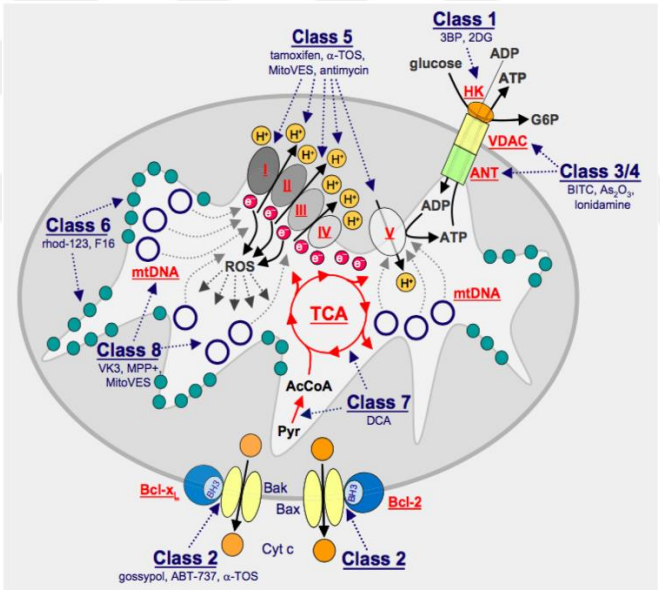

Figure 2.15. Mitocans. [36]

Mitocans of Class 8 target mtDNA, and cause destabilization of mtDNA either directly or indirectly. Thus, cell death occurs due to destabilization of mtDNA. For instance, 1-methyl-4-phenylpyridinium (MPP^+) directly interacts with mtDNA and destabilizes the mitochondrial D-loop. The structure of D-loop includes the sequence needed for replication. Therefore, mtDNA replication is consequently affected by MPP^+ [38]. Another agent that is included into Class 8 mitocans is known as polγ inhibitors. Polγ inhibitors for example vitamin K3 (vit K3, menadione) destabilize the functioning

of mtDNA by inhibiting the activity of polγ selectively [39]. Thus, apoptosis is triggered due to the destabilized mtDNA replication and the mtBER pathway is also affected. The last agent found in Class 8 mitocans known as MitoVES. MitoVES is the abbreviated form of mitochondrially targeted vitamin E succinate. MitoVES could either modulate the mtDNA directly or indirectly due to the ROS generation [38].

DNA repair deficiency often causes cancer. Synthetic lethal relationship between some of the genes/proteins occurs in different DNA repair pathways. [40]. Therefore, the viability of a cell is affected by the synthetic lethal interaction between two genes. The synthetic lethality means that both genes should be mutated for cell death as shown in Figure 2.16. Otherwise, viability of the cell can continue if one of these genes is active [41].

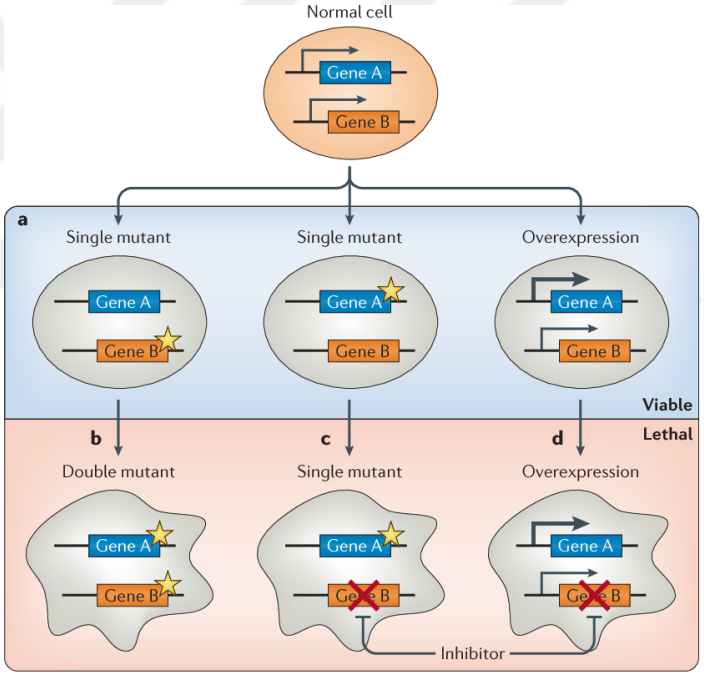

Figure 2.16. Mechanism of synthetic lethality. [41]

It has been found that MLH1 plays the crucial role in mitochondrial MMR. Almost 15-17% of colorectal cancer has MMR and MLH1 deficiency [42]. Thus, the viability of the cell is provided by BER pathway. Accordingly, the inhibition of polγ that involves in the BER pathway causes cell death [43].

As shown in Figure 2.17 the silenced polγ is synthetically lethal with mutated *MLH1*. The occurrence of oxidative DNA damage cannot be repaired. That's why mitochondrial 8-oxoguanine (8-oxoG) lesions accumulate in mitochondria and apoptosis is triggered [42].

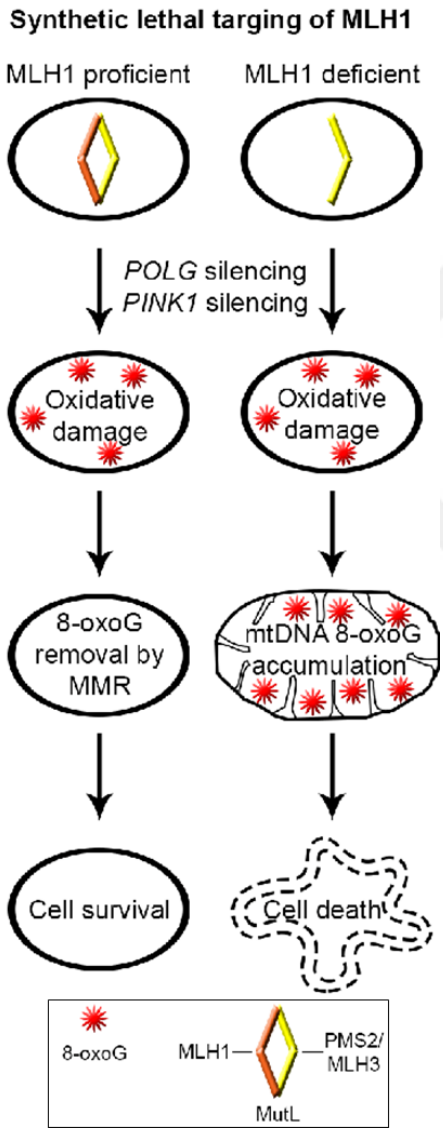

Figure 2.17. The synthetic lethal relationship between MLH1 and polγ. [42]

2.5. Tools for Genome Editing

The genetic information of living organisms can be modified by using genome editing. Genome editing is a powerful tool that uses programmable nucleases to make a change in targeted way [44]. It has been found that the endogenous repair mechanism of a cell can be triggered by double strand breaks (DSBs). A cell uses two major pathway for repairing these sites which are known as homology-directed repair (HDR) and non-homologous end-joining (NHEJ). Those repair systems can be used in a site-specific way by targeting DSBs [45]. For this purpose, many gene editing tools have been developed like zinc-finger nucleases (ZFNs), transcription activator-like effector nucleases (TALENs) and clustered regularly interspaced short palindromic repeats (CRISPR) [46].

2.5.1. Zinc Finger Nucleases

In 1996, a site-specific nuclease was discovered as a genome editing tool called as zinc finger protein. As shown in Figure 2.18, ZFNs work together with the FokI endonuclease and cleaves the DNA [47]. Two ZFNs needed for the opposite strands of DNA in order to trigger the DSB since FokI endonuclease performs its function as a dimer. Also, each finger of a ZFN could recognize three nucleotides. For instance, in Figure 2.18, three-fingered protein is bound to nine nucleotides [48].

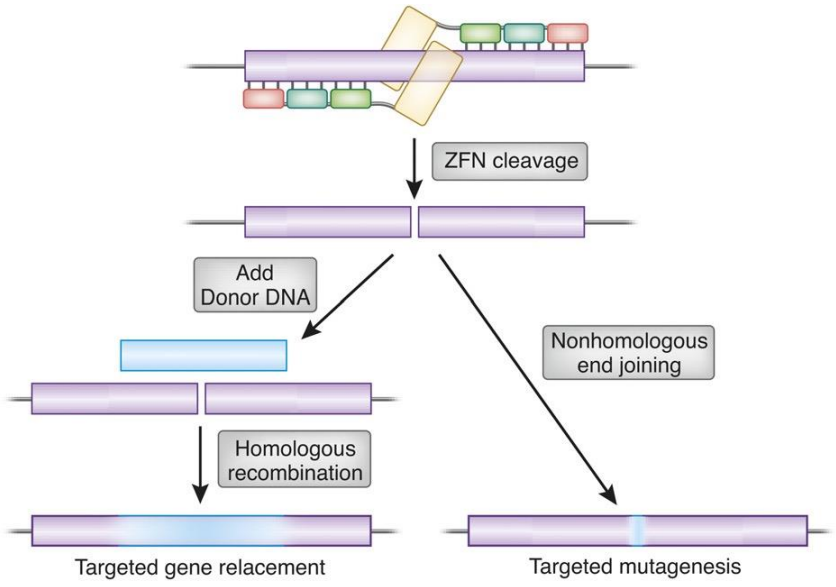

Figure 2.18. Genome engineering by ZFNs. [48]

Unfortunately, this technology has several disadvantages. It is very complex and expensive to construct the protein domain. Also, the interaction between protein domains could be inappropriate. Thus, for genome editing new technologies have been actively searched [47].

2.5.2. Transcription Activator-Like Effector Nucleases

In 2007, transcription activator-like effector (TALE) proteins were demonstrated as an alternative for programmable DNA-binding proteins. TALE proteins recognize adjacent DNA sequences like it was mentioned in ZFNs with only one difference. TALE proteins are able to bind to a single nucleotide as shown in Figure 2.19 [47, 49]. TALE proteins are also coupled with FokI endonuclease for the recognition of the targeted sequence [47].

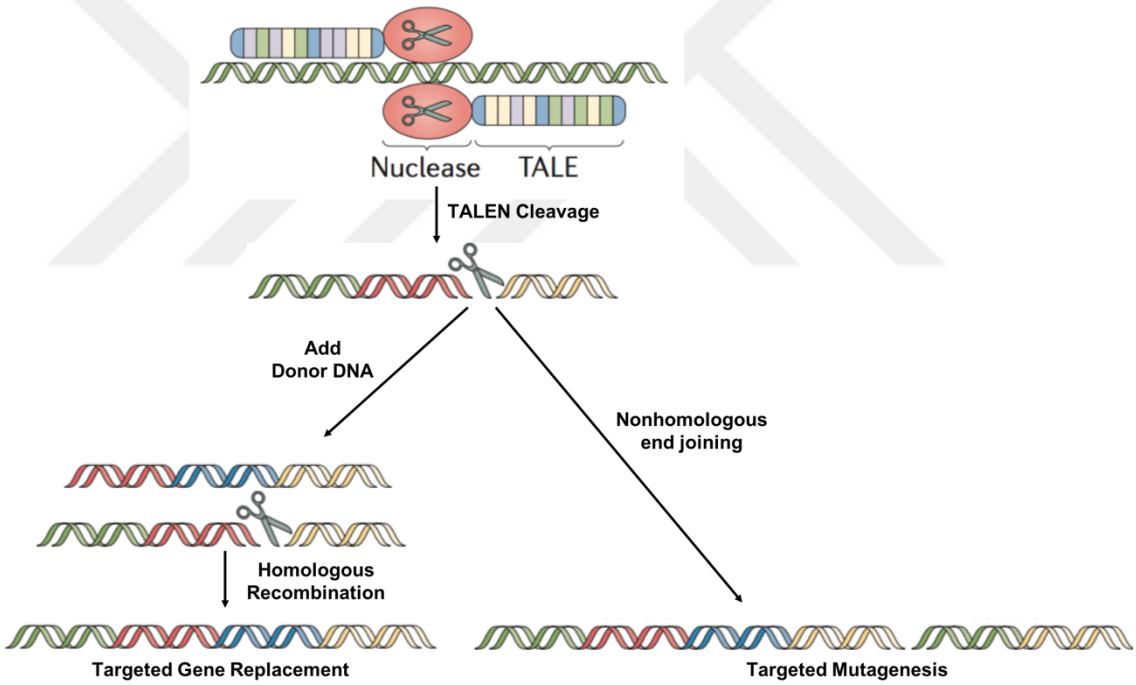

Figure 2.19. Genome engineering by TALENs. [50]

Since TALE proteins can bind to a single nucleotide, the gene editing technology with TALENs creates a lot of flexibility for the recognition-site [50]. However, TALENs also have limitations. Target sequence should have thymine at the 5'end in order TALE proteins perform their function appropriately [47].

2.5.3. CRISPR/Cas System

The most recent gene editing technology was discovered in 2009 and known as CRISPR [47]. CRISPR is the abbreviated form of **C**lustered **R**egularly-**I**nterspaced **S**hort **P**alindromic **R**epeats. It is considered as the most efficient gene editing tool in compared to the other tools discovered [51]. Thus, CRISPR is a powerful tool since specific genomic loci can be targeted by it, whereas the working principle of ZFNs and TALENs have based on protein-DNA interactions [52].

CRISPR/Cas system is divided into three major types as Type I, Type II, and Type III. The characterization between the types of CRISPR/Cas system is provided by a specific protein called as CRISPR-associated (Cas) protein. Cas proteins are composed of two major groups. One of the groups is core proteins such as Cas1 or Cas2 and the other group of Cas provides the differentiation between the CRISPR/Cas systems. These proteins are known as signature proteins and type I, II, and III, includes Cas3, Cas9, and Cas10, respectively [53].

The type II CRISPR system is the widely used CRISPR system since it is highly efficient and simple. The system is composed of two basic components called as a guide RNA (gRNA) component and a Cas9 nuclease. As the name implies gRNA provides the recognition of target sequence. It has two subunits known as CRISPR RNA (crRNA) and trans-activating crRNA (tracrRNA, trRNA). Cas9 is a nuclease that plays a role in unwinding of dsDNA. It is activated by the complex of crRNA and tracrRNA. Then, the whole complex has ability to recognize the protospacer adjacent motif (PAM) which is found at the end of the targeted DNA sequence. Thus, PAM is a marker for the recognition of the right sequence. Otherwise, the targeted DNA sequence could not be cleaved by the Cas9. PAM should have a sequence like -NAG or -NGG [54]. The targeted DNA sequence is composed of 20 nucleotides and the PAM sequence should immediately follow the target DNA sequence. Therefore, PAM sequence should be taken into consideration during the selection of targeted genomic loci and also the off-target activity should be minimized. As shown in Figure 2.20, gRNA and Cas9 form an complex (Cas9:gRNA complex) in order to find the targeted DNA sequence. As it was mentioned before PAM is used as a selection marker for Cas9:gRNA complex. As soon as Cas9:gRNA complex reaches to its target, a DSB is mediated by Cas9 approximately three base pairs later from the PAM sequence. Then, either HDR or NHEJ is stimulated for genome editing. The DNA repair mechanisms cause random indel mutations at the

binding site of the Cas9:gRNA complex. Frameshifts can appear as a result of indel mutations that occurred within the coding region of the gene, and then a premature stop codon can be created which may result in gene knock-out [55].

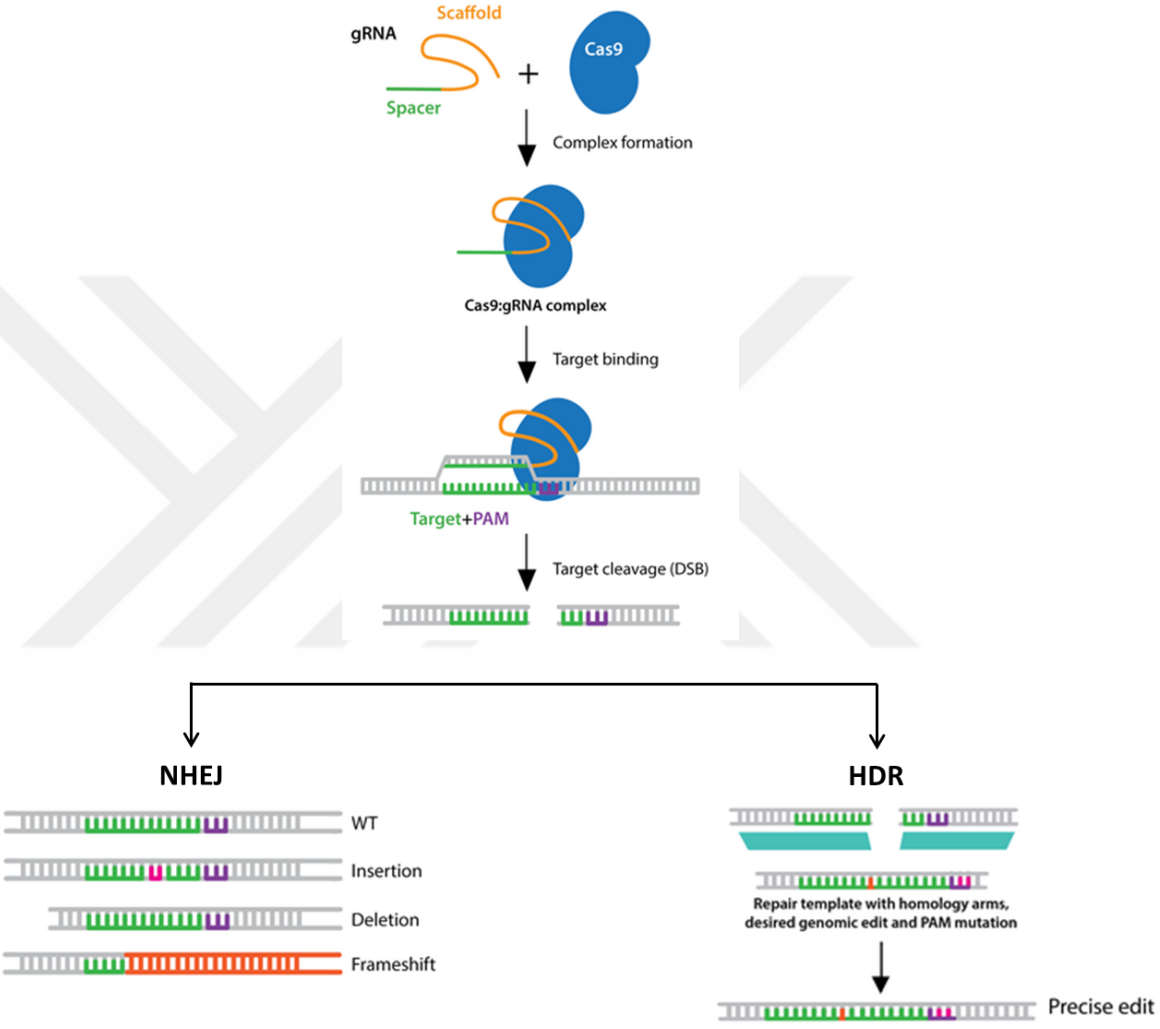

Figure 2.20. Working principle of CRISPR/Cas9 system. gRNA, guide RNA contains scaffold (orange) and spacer (green) sequences. Cas9, CRISPR-associated 9 enzyme (blue). The combination of gRNA and Cas9 is called as Cas9:gRNA complex. PAM, protospacer adjacent motif provides selectivity for target binding site. The cleavage of target results in double-strand break (DSB). This DNA damage is repaired either by non-homologous end-joining (NHEJ) or homology-directed repair (HDR). [56]

3. MATERIALS AND METHODS

3.1. Design of CRISPR/Cas9 System

Two 20 nucleotide long CRISPR sequences (Crispr#1 and Crispr#6) were designed that target catalytic subunit of polγ by using tools: CRISPR Design (http://crispr.mit.edu) and CRISPOR (http://crispor.tefor.net). The *polγ* gene sequence was obtained from Ensemble Genome Browser (ENSG00000140521) and NCBI (GRCh38). In order to design oligodeoxynucleotide, CLC Main Workbench 8 from QIAGEN Bioinformatics was used (Figure 3.1 and Table 3.1).

Figure 3.1. Amplification region of polγ; PCR product size = 668 bp. The specific regions are shown by arrows: forward and reverse primers (pink), start codon (yellow), targeted site by Crispr#1 or Crispr#6 (blue), restriction enzyme (HpyCH4III) cut site (coral).

Table 3.1. List of Oligodeoxynucleotides

Name of Oligodeoxynucleotide	Sequence 5'→ 3'	Purpose of Use
Cas9 reverse	TAT GTA ACG GGT ACC TCT AGA GCC	Sequencing primer of pSpCas9(BB)-2A-Puro
polγ forward	TTG GGG ACG CAG TAA ATG C	Genotyping
polγ reverse	AGT GCT GGT CCA GGT TGT C	Genotyping
Crispr#1 top	CAC CGA AGG TGG CCG GCG CCA CCG T	pSpCas9(BB)-2A-Puro Cloning
Crispr#1 bottom	AAA CAC GGT GGC GCC GGC CAC CTT C	pSpCas9(BB)-2A-Puro Cloning
Crispr#6 top	CAC CGA ACC GGC CCT GGC CCG ACG G	pSpCas9(BB)-2A-Puro Cloning
Crispr#6 bottom	AAA CCC GTC GGG CCA GGG CCG GTT C	pSpCas9(BB)-2A-Puro Cloning

3.2. Bacterial Cell Culture

3.2.1. Preparation of competent bacteria using $CaCl_2$ method

The day before the experiment, 100 μL bacteria from the competent bacteria (DH5α) stock was inoculated to 50 mL of LB broth (20g of LB (Sigma, #L7658-1KG) dissolved in 1L ddH_2O and then autoclaved.) and mixed for 16 h in a shaker (Biosan, #ES-20/60) at 180 rpm at 37°C. Then, 4 mL of the bacterial culture was introduced into 400 mL of LB broth and mixed at 180 rpm at 37°C until the optical density (OD) of the culture became 0.375 nm at 590 nm (Hitachi spectrophotometer, #U-1900). During this incubation step, working solution (composed of $CaCl_2$, MP Biomedicals, #195088; PIPES, Sigma, #P6757; Glycerol, Sigma, #15524-1L-R) was prepared and the ingredients used for this solution is shown in Table 3.2.

Table 3.2. Ingredients of Working Solution

Reagents	Stock Conc.	Final Conc.	Volume
$CaCl_2$	2 M	0.06 M	15 mL
PIPES, pH 7.0	0.5 M	0.01 M	10 mL
Glycerol	87%	15%	86 mL
ddH_2O	-	-	Up to 500 mL

As soon as culture was reached to 0.375 nm at 590 nm, it was aliquoted into eight pre-chilled falcon tubes equally. Then, the falcon tubes containing the bacterial culture were incubated on ice for 5-10 minutes. During incubation, the tubes were inverted occasionally to obtain homogeneous culture, and then centrifuged at 3500 rpm, at +4^{o}C for 10 minutes. At the end of centrifugation, supernatant was discarded. Pellets were dissolved in 10 mL of working solution and the mixture was incubated on ice for 30 minutes. Tubes were centrifuged at 3500 rpm, at +4^{o}C for 5 minutes and the pellets were resuspended in 2 mL of working solution. Finally, 200 μL of the mixture was aliquoted and immediately snap-frozen in liquid nitrogen. Prepared competent bacteria were stored at -80^{o}C.

3.2.2. Inoculation and Growth of Bacteria

For the inoculation and growth of bacteria LB broth and LB agar were used. LB agar is an autoclaved semi-solid growth medium for bacteria and it is composed of mixture of 20 g of LB and 15 g of agar (Sigma, #05039) in 1 L of ddH_2O. Then, ampicillin (Sigma, #A9518, stock concentration: 100 mg/mL) was added into the cooled mixture with 1:1000 dilution (in this case 1 mL of 100 mg/mL ampicillin was added per liter). Approximately, 10 mL of ampicillin containing LB agar was introduced into sterilized petri dishes and left for polymerization at room temperature. The polymerized plates were stored at +4^{o}C upside down. The enhancement of bacteria grown on the agar plate was provided by inoculating the desired bacteria into LB broth containing ampicillin with 1:1000 dilution.

3.2.3. Construction of vector and transformation

pSpCas9(BB)-2A-Puro (Puro) plasmid (Addgene, #62988) was used as a cloning backbone for oligodeoxynucleotide duplexes (Crispr#1 and Crispr#6). The structure of Puro plasmid is shown in Figure 3.2. Puro plasmid includes two recognition sites for BbsI restriction enzyme. Therefore, the digestion of Puro plasmid by BbsI restriction enzyme is advantegeous. After digestion it loses both of its recognition sites. That's why it provides direct insertion of annealed oligodeoxynucleotide duplexes. Also, it has a size of 9,175 bp.

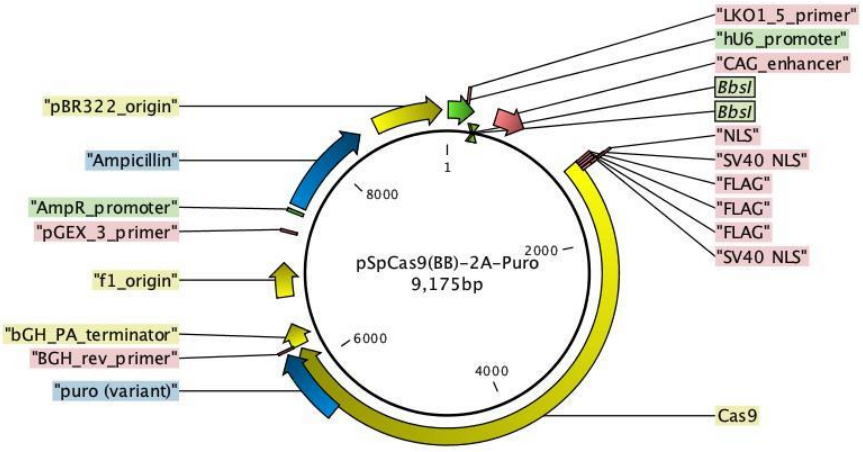

Figure 3.2. Plasmid map of pSpCas9(BB)-2A-Puro [55]

As it was mentioned at Section 3.1, in this thesis study two separate CRISPRs were designed. First, designed oligodeoxynucleotides were converted to double strand by an annealing reaction. The annealing reaction mixture was composed of 10X T4 DNA Ligase buffer (NEB, #M0202S) and T4 Polynucleotide Kinase (T4 PNK, NEB, #M0201S). The ingredients of the constructed annealing reaction and conditions were summarized in Table 3.3 and Table 3.4, respectively.

Table 3.3. Annealing Reaction

Reagents	Amount (μL)
Top oligo [100 μM]	1
Bottom oligo [100 μM]	1
10X T4 DNA Ligase Buffer	1
T4 PNK	1
ddH_2O	6
Total	10

Table 3.4. Annealing Reaction Conditions

Temperature	Time
37^oC	30 min
95^oC	5 min
Ramp Down to 25^oC	5^oC/min
4^oC	∞

As soon as the top and the bottom strands of the designed oligodeoxynucleotides were annealed; the obtained products from the annealing reaction were 1:200 diluted with ddH_2O. Then, diluted oligodeoxynucleotide duplexes were ligated to plasmid

called as pSpCas9(BB)-2A-Puro (Puro, Addgene, #48139). The ligation reaction was also included 10 mM 1,4-Dithiothreitol (DTT, Sigma, #3483-12-3), 10 mM Adenosine 5'-triphosphate (ATP, NEB, #P0756S), BbsI (NEB, #R0539S) and T4 DNA Ligase (NEB, #M0202S). Ingredients of the constructed ligation reaction are summarized at Table 3.5 and Table 3.6.

Table 3.5. Ligation Reaction

Reagents	Volume (μL)
pSpCas9(BB)-2A-Puro (100 ng/μl)	1
Diluted oligodeoxynucleotide duplex	2
10X T4 DNA Ligase Buffer	2
10 mM DTT	1
10 mM ATP	1
BbsI	1
T4 DNA Ligase	0.5
ddH_2O	11.5
Total	20

Table 3.6. Ligation Reaction Conditions

Temperature	Duration	# of Cycles
37^oC	5 min	6 Cycles
21^oC	5 min	
4^oC	∞	

In order to get rid of the free oligodeoxynucleotide duplexes T5 exonuclease treatment was applied to the ligation reaction by using combination of 10X NebBuffer 4 (NEB, #B7004S), ATP, and T5 exonuclease (NEB, #M0363S) (Table 3.7).

Table 3.7. T5 Exonuclease Treatment Reaction

Reagents	Amount (μL)
Ligation Rxn	20
10X NebBuffer 4	3
ATP	3
T5 Exonuclease	1
ddH_2O	3
Total	30

Table 3.8. T5 Exonuclease Treatment Reaction Conditions

Temperature	Duration
37°C	30 min
➔ Add 3.85 µl EDTA (100mM) and 1.15 µl ddH_2O at the end of 30 min	
70°C	30 min

As soon as T5 exonuclease treatment was finished, the transformation protocol was started by transforming 1 µL end-product of T5 exonuclease treatment reaction into 200 µL of competent bacteria (which was prepared according to Section 3.2.1). Then, tubes were incubated on ice for 25 minutes and then samples were incubated at 42°C for 90 seconds. By this manner, bacteria can take the given product taken from T5 exonuclease treatment. In order to reclose the pores formed through the heat shock, samples were incubated on ice for 1 minute. Then, the growth of bacteria was supplied by introducing them into 37°C waterbath for 35 minutes. At the end of incubation, centrifugation was done at 13000 rpm for 30 seconds. To resuspend the pellet approximately 100 µL of supernatant was left in the tubes. Then, the entire product was cultured on an agar plate. Incubation was done for 16 hours at 37°C. The day after transformation, the bacterial colonies were collected from the agar plate and inoculated into 3 mL LB broth w/amp for plasmid DNA isolation by using PureLink Quick Plasmid MiniPrep Kit. Then, inoculation of the bacterial culture was used 100 mL (PureLink HiPure Plasmid MidiPrep Kit was used) in order to obtain higher DNA yield for further analysis.

3.2.4. Plasmid DNA isolation by alkaline lysis solution

The selected bacteria were grown in 3 mL of LB broth with ampicillin for 16 hours. Then, 1.5 mL of bacterial culture was aliquoted into eppendorf tubes and 885 µL of them was separated for glycerol stocks (Sigma, #15524-1L-R) stocks (115 µL 87% glycerol + 885 µL bacteria) and stored at -80°C. For the plasmid DNA isolation, the tubes separated for isolation were centrifuged at 14800 rpm, at +4°C for 30 seconds. After centrifugation, supernatants were discarded and pellets were resuspended in 100 µL of ice-cold Alkaline Lysis Buffer I (50mM glucose, 25mM Tris-Cl pH 8.0, 10mM EDTA pH 8.0 (Invitrogen, #15575-020)). Then, 200 µL of freshly prepared Alkaline Lysis Buffer II (0.2N NaOH, 1% sodium dodecyl sulfate (SDS; Sigma, #151-21-3)) was added into each tube. The lysis step was finished by the addition of 150 µL Alkaline

Lysis Buffer III (3M potassium acetate, 11.5% glacial acetic acid, ddH_2O) and then tubes were incubated on ice for 4 minutes. At the end of incubation, samples were centrifuged at 14800 rpm, at $+4^oC$ for 5 minutes. During centrifugation 900 μL of absolute ethanol was added into clean tubes. After centrifugation supernatant of samples were introduced into 900 μL of absolute ethanol. Then, tubes were inverted for 3 times. All samples were centrifuged again at 14800 rpm, at $+4^oC$ for 5 minutes. At the end of centrifugation, supernatants were discarded and 1 mL of 70% ethanol was added into each tube for washing step. Plasmid DNA pellet was obtained by centrifugation at 14800 rpm, at $+4^oC$ for 2 minutes. After centrifugation supernatant was discarded and tubes were air-dried. Finally, pellets were dissolved in 50 μL TE Buffer mixed with RNase.

3.2.5. Plasmid DNA isolation by PureLink Quick Plasmid MiniPrep Kit

Plasmid DNA isolation was performed using PureLink Quick Plasmid DNA MiniPrep Kit according to the manufacturer's protocol (Invitrogen, #00471207).

3.2.6. Plasmid DNA isolation by PureLink HiPure Plasmid MidiPrep Kit

Plasmid DNA isolation was performed using PureLink HiPure Plasmid MidiPrep Kit according to the manufacturer's protocol (Invitrogen, #00402938).

3.2.7. Verification of CRISPR plasmids by Sanger sequencing

The validation of inserted 20 nt long CRISPR sequences (Crispr#1 or Crispr#6) was performed using Applied Biosystems Sanger Sequencing 3500 Series Genetic Analyzers in MedSanTek Laboratories, Istanbul, Turkey. Cas 9 reverse primer was used for verifying the sequences of each colony.

3.3. Mammalian Cell Culture

3.3.1. Thawing frozen cells and growth of cells

HCT116 and HCT116_Chr3 cell lines were taken from liquid nitrogen tank and cryovials were heated at 37^oC water bath until the cell mixture inside the tube melted. HCT116 and HCT116_Chr3 cell lines were kind gifts from Dr. Thomas Kunkel (National Institutes of Health (NIH)/National Institute of Environmental Health

Sciences (NIEHS), USA). As soon as, it was melted 1 mL of complete medium of DMEM/F-12 (Gibco, #31330-038) containing 10% Fetal Bovine Serum (FBS, ThermoScientific, #10270106), 1% Penicillin/Streptomycin (LifeTech, #15140122) was added into it and all of the mixture was introduced into petri dish filled with suitable amount of complete medium. Then, plates were left in 37^{o}C, 5% CO_2 incubator.

3.3.2. Optimized polyethylenimine (PEI) transfection and analysis of transfection efficiency

In order to start the transfection process, Crispr#1 (2.187 μg/μL), Crispr#6 (1.745 μg/μL), Puro (2.000 μg/μL) and pSpCas9(BB)-2A-GFP (GFP, 2.000 μg/μL) were used. The day before the transfection, 1x10^{6} cells from 90-95% confluent plates of HCT116 and HCT116_Chr3 cell lines were cultured into 10 cm tissue culture plates. As soon as, the plates were reached to 40-50% confluency, the transfection process was performed. For this purpose, 15 μg of plasmid DNA per sample was introduced into 1 mL of serum-free DMEM/F-12. Then, 1 μg/μL PEI (Polysciences, #23966-2) was added with 1:4 ratio of plasmid DNA (μg) to PEI (μg) into the prepared mixture and vortexed immediately. In order to obtain PEI and plasmid DNA complexes, mixtures were incubated for 15 minutes at room temperature. Finally, the incubated mixtures were added into the desired cells drop by drop and incubated at 37^{o}C, 5% CO_2 incubator for 16 hours. The day after transfection process, medium of cells were aspirated and fresh medium was added. Complete medium of DMEM/F-12 was mixed with sodium pyruvate (100mM, LifeTech, #11360-039) and uridine (100mM, Sigma, #U3003-5G) for Crispr#1 and Crispr#6 transfected HCT116 cells and additionally geneticin (400 μg/mL) was included into medium of HCT116_Chr3 cells. After 40 h from transfection, GFP transfected cells lines were visualized by fluorescence microscope (ZEIS, Vert.A1) in order to determine the transfection efficiency. As the transfection efficiency was high enough, puromycin (Sigma, #P9620) mixed in complete DMEM/F-12 was added into the cells for selection.

3.3.3. Split of transfected cells into 96-well plates (or obtaining single colonies)

Transfected HCT116 and HCT116_Chr3 cells obtained from optimized PEI transfection were splitted into 96-well plates by trypsinization (Trypsin-EDTA (0.05%)). Then, the cell pellet was obtained by centrifugation at 300xg for 3 minutes at

room temperature. The cell pellet was re-suspended in 10 mL of DMEM/F-12. Then, the cell was counted by using hemocytometer and diluted in DMEM/F-12 with a final concentration of 1 cell per 200 μL were plated into 96-well plates. Then, plates were placed in 37^{o}C, 5% CO_2 incubator. As soon as, colonies were visible, single colonies were transferred into 24-well plates. As soon as cells in 24-well plates reached to 90-95% confluency, half of the cells were separated as cell pellets for total DNA isolation and the other half of them was frozen for further analysis. Isolated DNAs were used for genotyping. Genotyping was performed by PCR (Veriti 96-well Thermal Cycler, #4375786) and agarose gel electrophoresis (Major Science, #ME15-7-10-15). As a result of genotyping analysis, some of the single colonies were selected and grown in cell culture conditions. Half of the cells were collected for cell extract preparation and the other half was cryopreserved.

3.4. Analysis of Efficiency of Genome Targeting

3.4.1. Total DNA isolation

Total DNA isolation for entire samples of pool and single colonies were done with the same procedure. The pellets obtained from cells were used. The tail lysis buffer (500 μL) (100mM Tris pH 8.0 (BioRad, #1610716), 100mM sodium chloride (NaCl, Sigma, #13423), 10mM EDTA pH 8.0, 0.5% SDS) were introduced directly to the pellets and 10 μL of Proteinase K (Roche, #745723) was added. Incubation was applied for 90 minutes at 55^{o}C. At the end of incubation, 250 μL of 5M NaCl was added into each tube. Tubes were inverted for twenty times and then incubated on ice for 10 minutes. Centrifugation was done for 20 minutes at 3000 rpm and +4^{o}C. Supernatant obtained after centrifuge was introduced into a clean eppendorf tube. Then, 650 μL of isopropanol (Sigma, #24137) was added into each sample and mixed by converting up and down. Samples were incubated at room temperature for 15 minutes. At the end of incubation, centrifugation was done at maximum speed (13000 rpm) and at room temperature for 10 minutes. After centrifugation, supernatant was discarded. Pellet obtained after this step contains DNA. Washing step was done by mixing the pellet with 1 mL of 70% ethanol (Sigma, #32221-2.5L). Then, ethanol was removed from the sample (DNA) by centrifugation at maximum speed and room temperature for 10 minutes. Tubes were dried for approximately 5 minutes in order to be sure that whole

ethanol had been removed from the tube. Finally, DNA was resuspended with desired volume (which could be 50/100/200 μL) of TE buffer (Invitrogen, #00431008).

3.4.2. Constructing polymerase chain reaction by using isolated total DNAs

Targeted region of *polγ* gene was amplified by using designed primers shown at Section 3.1 by the polymerase chain reaction (PCR) procedure. The reaction mixture for amplification was composed of betaine (Sigma, #B-0300), standard buffer (NEB, #B9014S), dNTP (Applied Biosystems, #1609158), forward primer (Metabion International AG), reverse primer (Metabion International AG) and DNA Taq Polymerase (NEB, #M0320S). Ingredients and conditions used for PCR were summarized in Table 3.9 and Table 3.10, respectively.

Table 3.9. PCR Ingredients

Chemical Added	Amount (μL)
Betaine	6
Buffer (w/Mg^{2+})	2,5
dNTP (10 mM)	0,5
Forward Primer (10 mM)	2
Reverse Primer (10 mM)	2
DNA Taq Polymerase	0,125
DNA	1
ddH_2O	10,875
TOTAL	25

Table 3.10. PCR Conditions

Step	Temperature	Duration	
Denaturation	95°C	4 min	
Annealing	95°C	30 sec	x 30 cycles
	62°C	30 sec	
	72°C	45 sec	
Elongation	72°C	5 min	
Hold	4°C	∞	

3.4.3. RFLP assay

Both CutSmart Buffer (NEB, #B7204S) and HpyCH4III (NEB, #R0618S) restriction enzymes were obtained from NEB. All conditions and ingredients needed for RFLP assay was summarized in Table 3.11 and Table 3.12.

Table 3.11. Construction of Uncut and Cut Reactions

Uncut Reaction		Cut Reaction	
PCR Product	12 μL	**PCR Product**	12 μL
CutSmart Buffer	1.5 μL	**CutSmart Buffer**	1.5 μL
HpyCH4III	--	**HpyCH4III**	0.2 μL
ddH_2O	1.5 μL	**ddH_2O**	1.3 μL
TOTAL	15 μL	**TOTAL**	15 μL

Table 3.12. Incubation Conditions for RFLP

Temperature	Duration
37^oC	3 h
65^oC	20 min
4^oC	∞

3.4.4. Preparation of cell extract

Cells that were determined as CRISPR worked properly were cultured to 6 cm cell culture plates. When the cells reached to suitable confluency (~70%), all of them were transferred to 10 cm tissue culture plate in order to obtain extra amount of cells. As soon as cells became confluent, the pellet was obtained from all of the plates. During this procedure all of the steps were done on ice. In order to obtain pellet from plates, firstly medium was aspirated and cells were washed with 5 mL of DPBS (1X) for twice. Then, 1 mL of Trypsin-EDTA (0.05%, 1X) was added into all the plates and incubated at 37^oC, CO2 incubator for 2 minutes. At the end of incubation, Trypsin-EDTA was inactivated by addition of 8 mL of DMEM/F-12 with FBS into the plates. Cells were centrifuged at +4^oC, 600xg for 5 minutes. After centrifugation supernatant was aspirated. The cell pellet was dissolved in 1 mL of cold DPBS (1X) and transferred to eppendorf tube. All of the samples were again centrifuged at +4^oC, 600xg for 5 minutes. Supernatant obtained after centrifugation was again aspirated and cell pellet was obtained. In order to prepare cell extract RIPA buffer was prepared. It was composed of Tris-HCl (Tris, BioRad, #1610716; HCl, Sigma, #30721-2.5L), NaCl (Sigma, #13423), EDTA, sodium fluoride (NaF, Merck, #106441), sodium orthovanadate (Na_3VO_4, Merck, #567540), NP-40 (Pierce, #PI-85124), TritonX-100 (Sigma, #X100-500ML), phenylmethylsulphonyl fluoride (PMSF, Roche, #10837091001), 1,4-Dithiothreitol

(DTT), protease inhibitor (Roche, #11836170001). The ingredients for preparation of RIPA buffer is summarized in the following Table 3.13.

Table 3.13. 5 mL RIPA Buffer Preparation

Stock Concentration	Reagent	Final Concentration	For 5 mL
1 M	Tris-HCI	50 mM	250
5 M	NaCl	150 mM	150
0.5 M	EDTA	1 mM	10
200 mM	NaF	1 mM	25
100 mM	Na_3VO_4	1 mM	50
20%	NP-40	0.5%	125
20%	TritonX-100	2%	125
50 mM	PMSF	0.5 mM	50
1 M	DTT	1 mM	5
50X	Protease inhibitor	1X	100
	ddH_2O		4110

The pellets were dissolved in the proper amount of RIPA buffer and then incubated on ice for 30 minutes. At the end of the incubation, samples were centrifuged at +4^{o}C, 14000xg for 15 minutes. The supernatants were placed into a clean eppendorf tube. Cell extracts was prepared. All of the flash-frozen cell extract samples were stored at -80^{o}C.

3.4.5. Bradford assay

First of all, in order to determine the concentration protein in the samples prepared at Section 3.4.5, nine dilutions of protein standards (BSA; Cell Signaling, #9998S) were prepared between the ranges of 10 to 800 μg and then stored at -20^{o}C. The dilutions calculated for the protein (BSA) standards are summarized in the following Table 3.14.

Table 3.14. Preparation of Bradford Assay Protein Standards

BSA Stock (2mg/mL)	ddH_2O (μL)	BSA(mg/μL)	BSA (μg/mL)
1 μL	199	0.01	10
2 μL	198	0.02	20
4 μL	196	0.04	40
8 μL	192	0.08	80
10 μL	190	0.1	100
20 μL	180	0.2	200
40 μL	160	0.4	400
60 μL	140	0.6	600
80 μL	120	0.8	800

The Bradford reagent was brought to room temperature during the preparation of 96-well plate with distilled water, BSA standards, and samples. After introducing 5 μL of samples to the 96-well plate, warmed Bradford reagent (BioRad, #500-020S) was poured into the sterile reservoir and by the help of multi-channel pipette 250 μL of Bradford reagent was introduced into each well. In order to eliminate the effect of light the 96-well plate filled with samples closed by using styrofoam box and then incubated at dark for 5 minutes. During the incubation, plate reader (BioTek, Powerwave XS2) was prepared according to instructions. The absorbance value of the samples should not pass 1. If the absorbance values obtained from the device was above 1, dilutions were done accordingly. Finally, the result obtained from the device was transferred to the Microsoft Excel and graphic was drawn. The R^2 value obtained from the Microsoft Excel data should be equal/very close to 1.

3.4.6. Western blot analysis

First of all, 10% gel was prepared and poured between 0.75 mm glasses (BioRad, #1653311). In Table 3.15, the ingredients used for preparation of 10% gel is summarized and composed of 40% acrylamide/bisacrylamide (BioRad, #161-0148), 1M Tris pH 8.8, 10% ammonium persulfate (APS; Sigma, #7727-54-0), 10% SDS and tetramethylethylenediamine (TEMED; Sigma, #110-18-9).

Table 3.15. Ingredients needed for 10% Western Blot gel

Chemical Added	Amount of Chemical
ddH_2O	2.5 mL
40% acrylamide/bisacrylamide	1.25 mL
1M Tris, pH: 8.8	1.25 mL
10% SDS	50 μL
10% APS	50 μL
TEMED	50 μL

The amount of protein was determined by using Bradford Assay. Each sample's protein concentration was brought to equal amount which was 30 μg. Then, according to the determined concentration of protein amount of cell extract was calculated in terms of microliters and it was mixed by same amount (1:1) of 2X Laemmli Buffer (LB, BioRad, #1610737). The mixture was incubated at 95^{o}C for 5 minutes by using a heat block. At the end of incubation, samples were put on ice and loading of samples was

started. Loaded gel was run at 80V for 1.5 hours. Then, the gel was introduced to 1X Transfer Buffer (BioRad, #1610734). During this step, the membrane (PVDF/Nitrocellulose, BioRad, #170-4156) was put in methanol for 30 seconds. After 30 seconds, it was introduced into 1X Transfer Buffer for 5 minutes. Then, the transfer pack (BioRad, #170-4158) was put in 1X Transfer Buffer and placed into the cell of semi-dry blotter (BioRad, Trans-Blot Turbo). Gel was taken from the 1X Transfer Buffer and put onto the membrane. The sandwich mechanism designed was finished by putting wet (with 1X Transfer Buffer) Whatman filter paper at the uppermost part of the sandwich. Finally, the lid of the cell was closed and placed into the semi-dry blotter. The program was run according to the instructions (Choose: List → BioRad → 1 mini gel → mixed 1,3A - 2,5V – 15 minutes). Then, the membrane was placed into ~25 mL of 5% non-fat milk (BioRad, #170-6404) and incubated on the shaker (Witeg, RK-1D) for 1 hour at room temperature. At the end of incubation in 5% non-fat milk for 1 hour, primary antibodies (Polγ, Cell Signaling #13609S; β-actin, Cell Signaling #3700S) prepared in 5% non-fat milk was introduced onto the membranes and then incubated at +4^{o}C overnight. Then, the membrane was washed with 1X TBS-T (5M NaCl, 1M Tris pH 7.4 and 1% Tween-20- (Sigma, #P5727)) for 5 minutes three times in order to get rid of the primary antibody. As soon as washing step was finished secondary antibodies (anti-mouse (Cell Signaling, #7076S) or anti-rabbit (Cell Signaling, #7074S) with 1:5000 dilution) were added onto the membranes and incubated at room temperature for 1 hour. Then, membranes were washed with ~15 mL 1X TBS-T for 30 minutes three times. As washing steps were finished, detection reagents (FEMTO, ThermoScientific, #34095; ECL, ThermoScientific, #32132) were applied onto the membranes and screening was done by ChemiDoc (BioRad, ChemiDoc MP, Imaging system).

3.4.7. TA cloning

The desired region of the single cell total DNAs were amplified and run on an agarose gel electrophoresis. However, for this purpose low melting agarose (Bioshop, #AGA103.100) was used during the preparation of gel. Since there were primer dimers for all of the chosen samples, the bands obtained from the agarose gel electrophoresis were isolated by using PureLink Quick Gel Extraction Kit (Invitrogen, #00551630). Purified DNA products were cloned into pTZ57R/T plasmid according to InsTAclone PCR Cloning Kit (ThermoScientific, #00593025) protocol. According to the manufacturers protocol ligation reaction was summarized in the following Table 3.16.

Table 3.16. Ligation Reaction

Chemical Added	Amount of Chemical
Vector (pTZ57R/T)	3 μL
5X Ligation Buffer	6 μL
PCR Product (129 ng)	… μL **
ddH_2O (nuclease-free)	to 29 μL
T4 DNA Ligase	1 μL
Total	30 μL

** Each amount of samples was calculated according to their concentrations.

All of the chemicals written in the above Table 3.16 were mixed and a brief vortex was applied and span down. Then, samples were left for incubation for 1 hour at room temperature. During this step, 40 μL of X-Gal (Sigma, #B4252) and 40 μL of IPTG (Fermentas, #R0392) were added onto the LB agar plates and chemical were spread onto the plates by the help of glass beads. Then, plates were incubated at 37^{o}C incubator. As a final step, transformation was done by using the procedure explained at Part 3.2.3. Plasmid DNAs of the obtained blue colonies were isolated according to the procedure explained at Part 3.2.4.

3.4.8. Sanger sequencing done for targeted region of DNAs

DNA products cloned into the pTZ57R/T plasmid were isolated by using alkaline lysis protocol and the sequencing of the isolated plasmid DNAs were provided by MC Lab (https://www.mclab.com). Six of the colonies were chosen from the single colonies and for every single colony 16 samples of isolated plasmid DNA was sent. M13 Forward (-20) (Invitrogen, #N52002) was used as primer.

4. RESULTS

4.1. Verification of Oligodeoxynucleotides for Genome Editing of polγ by Sanger Sequencing

First of all, oligodeoxynucleotide pairs of Crispr#1 or Crispr#6 which target the *polγ* gene (Table 3.1) were annealed. Then, oligodeoxynucleotide duplexes were cloned into BbsI digested pSpCas9(BB)-2A-Puro (Puro) plasmid (Figures 4.1A and 4.1B). Puro plasmid has two recognition sites for BbsI. By this manner, when the oligodeoxynucleotide duplexes cloned into Puro plasmid, recognition sites of BbsI are lost. Then, Puro plasmids containing oligodeoxynucleotide duplexes were transformed into competent bacteria for plasmid DNA isolation. The isolated Crispr#1-Puro and Crispr#6-Puro plasmids were digested with BbsI restriction enzyme and run on 1% agarose gel electrophoresis to verify whether the oligodeoxynucleotides were inserted into Puro plasmid or not (Section 3.2.3). Annealed oligodeoxynucleotide duplexes also have no BbsI recognition site, so that Crispr#1 and Crispr#6 transfected plasmids cannot be digested by BbsI. Therefore, two bands are observed in Figure 4.1C. Figure 4.1C shows that the oligodeoxynucleotides are inserted into the Puro plasmid correctly. The cloning of the Crispr#1 or Crispr#6 was also verified by Sanger sequencing (Figure 4.1D). The sequencing result showed that Crispr#1 or Crispr#6 designs were truly cloned into Puro plasmid.

4.2. Analysis of Transfection Efficiency by Fluorescence Microscope

PEI transfection method was used to introduce plasmids into HCT116 and HCT116_Chr3 cell lines. The verification of the transfection efficiency was done by transfecting green fluorescent protein (GFP) into HCT116 and HCT116_Chr3 cell lines and 40 hours later from the PEI transfection, the excitation of GFP under fluorescence microscope was analyzed. Transfected plates were visualized under both transmitted light (TL) and reflected light (RL) in order to determine the cell viability and transfection efficiency. The green dots in Figures 4.2B and 4.2D indicate that the PEI transfection was done successfully. Thus, PEI transfection method was used for CRISPR/Cas9 transfection.

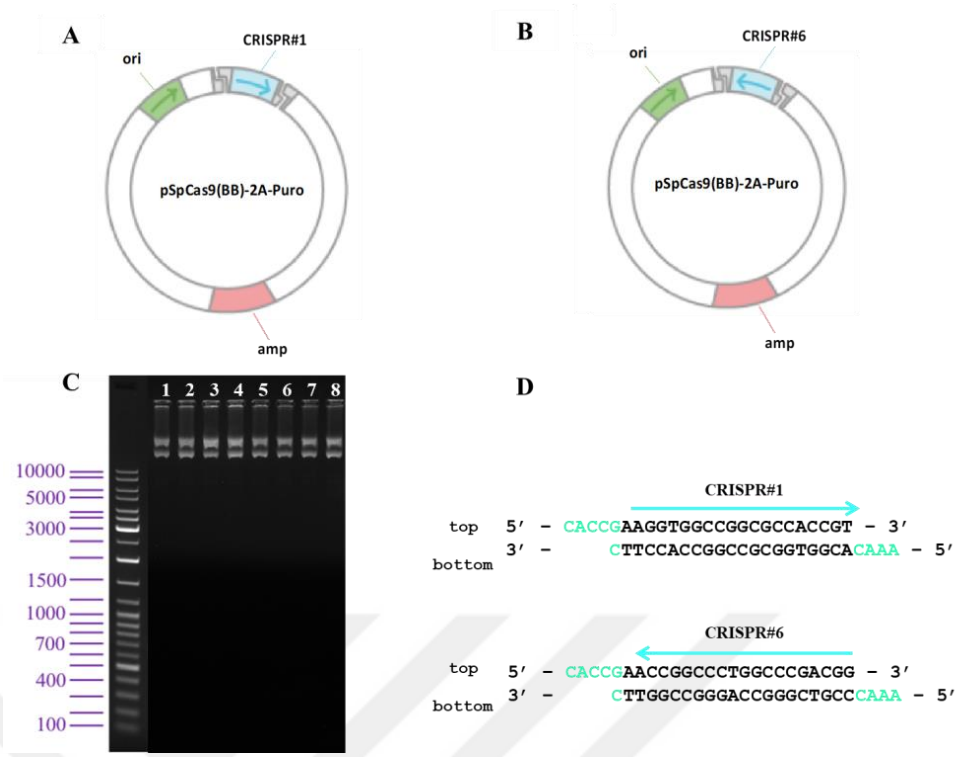

Figure 4.1. Insertion of Crispr#1 or Crispr#6 oligodeoxynucleotide duplexes into pSpCas9(BB)-2A-Puro plasmid. **A.** A representative image for insertion of Crispr#1 into Puro plasmid; **B.** A representative image for insertion of Crispr#6 to Puro plasmid; **C.** Agarose gel electrophoresis analysis of digested plasmids (lanes 1-4, plasmids of Crispr#1; lanes 5-8, plasmids of Crispr#6); **D.** Sanger sequencing analysis of both cloned Crispr#1and Crispr#6.

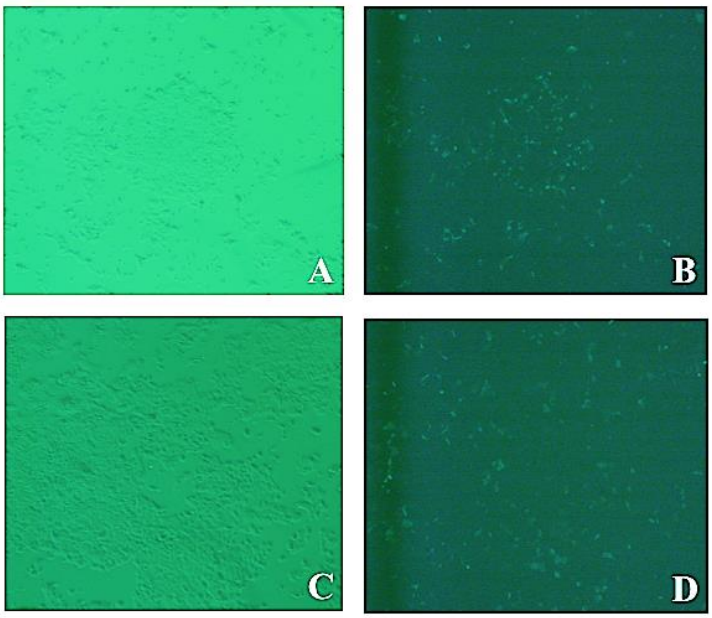

Figure 4.2. Image visualized by fluorescence microscope; **A.** HCT116 (visualized under TL), **B.** HCT116 (visualized under RL), **C.** HCT116_Chr3 (visualized under TL), **D.** HCT116_Chr3 (visualized under RL)

4.3. Verification of CRISPR/Cas9 Mutations of polγ in HCT116 and HCT116_Chr3 Cell Lines

Total DNA was isolated from Crispr#1 or Crispr#6 plasmid (Figure 4.1A and 4.1B) transfected pools of HCT116 and HCT116_Chr3 cell lines, and then verified by PCR. The PCR products run on agarose gel electrophoresis and the desired size of PCR products which is 668 bp was obtained (Figure 4.3). In Figure 4.3, lane 1 and lane 4 represent the transfected HCT116 and HCT116_Chr3 cell lines by empty Puro plasmid (mock) and named as HCT116-Puro and HCT116_Chr3-Puro, respectively. The band density of lane 1 is thicker than the density of lane 4. Therefore, the transfection efficiencies of HCT116 cell lines are better than the transfection efficiencies of HCT116_Chr3 cell lines. In addition, the transfection efficiency of HCT116_Chr3 cell lines for Crispr#1 or Crispr#6 (Figure 4.3; lanes 5-6) were less than Crispr#1 or Crispr#6 transfected HCT116 cell lines (Figure 4.3; lanes 2-3).

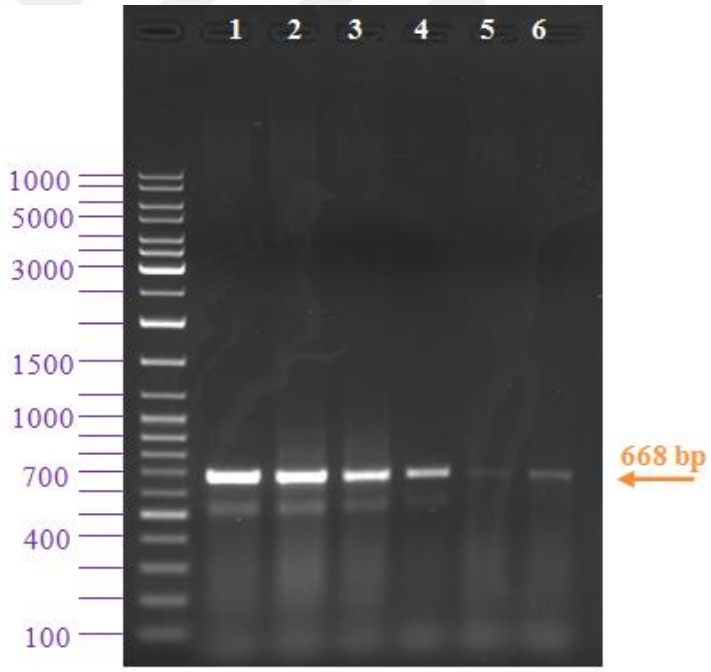

Figure 4.3. Agarose gel electrophoresis analysis of amplified PCR products by using total DNAs isolated from Crispr#1 or Crispr#6 transfected pools of HCT116 and HCT116_Chr3 cell lines as a template. Lane 1, HCT116-Puro; lane 2, HCT116-Crispr#1; lane 3, HCT116-Crispr#6; lane 4, HCT116_Chr3-Puro; lane 5, HCT116_Chr3-Crispr#1; lane 6, HCT116_Chr3-Crispr#6

As soon as the desired PCR products were obtained from the transfected pools (Figure 4.3), the RFLP analysis (digestion by HpyCH4III) was performed for screening CRISPR/Cas9-mediated mutant clones of HCT116 or HCT116_Chr3. The

quantification of mutations was done by evaluating the pattern of digestion (Figure 4.4). The lanes with odd number (Figure 4.4; lanes 1, 3, 5, 7, 9, 11) show the PCR products without RFLP. The lanes with even number (Figure 4.4; lanes 2, 4, 6, 8, 10, 12) show the digested PCR products. All of the digested PCR products give two smaller bands. In Figure 4.4 (lanes 2 and 8) show the digested samples of mocks. The transfected pools of CRISPR/Cas9-mediated mutant clones of HCT116 or HCT116_Chr3 cell lines include wild-type cells (two smaller bands; Figure 4.4; lanes 4, 6, 10, 12), heterozygous mutants and homozygous mutants stay as uncut (668 bp) (Figure 4.4; lanes 4, 6, 10, 12). Therefore, transfected pools of CRISPR/Cas9-mediated mutant clones of HCT116 or HCT116_Chr3 were used for the creating single cell colonies in order to select cell(s) containing only knockdown *polγ* gene.

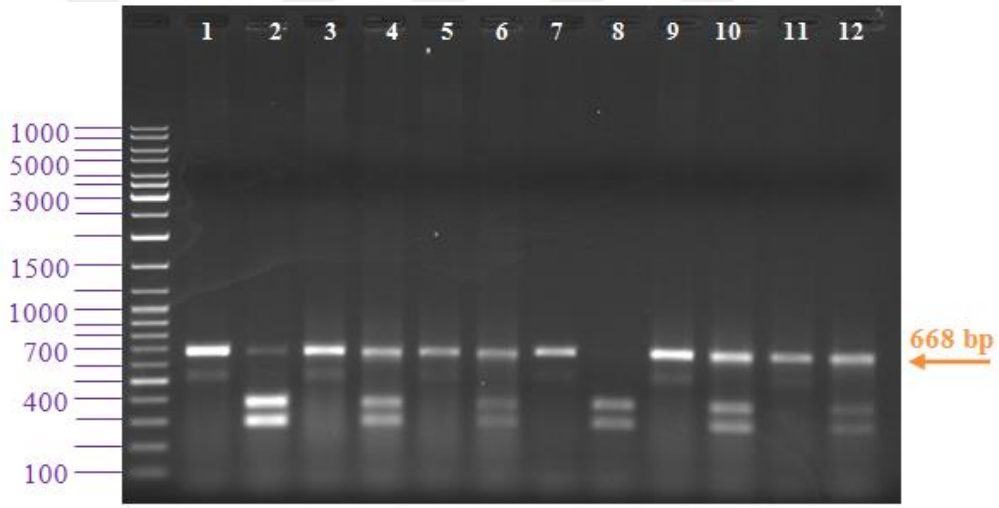

Figure 4.4. Agarose gel electrophoresis analysis of RFLP of amplified PCR products by using total DNAs isolated from Crispr#1 or Crispr#6 transfected pools as a template. Lane 1, HCT116-Puro-Uncut; lane 2, HCT116-Puro-Cut; lane 3, HCT116-Crispr#1-Uncut; lane 4, HCT116-Crispr#1-Cut; lane 5, HCT116-Crispr#6-Uncut; lane 6, HCT116-Crispr#6-Cut; lane 7, HCT116_Chr3-Puro-Uncut; lane 8, HCT116_Chr3-Puro-Cut; lane 9, HCT116_Chr3-Crispr#1-Uncut; lane 10, HCT116_Chr3-Crispr#1-Cut; lane 11, HCT116_Chr3-Crispr#6-Uncut; lane 12, HCT116_Chr3-Crispr#6-Cut

4.4. Verification of CRISPR/Cas9 Mutations of polγ in Single Colonies of HCT116 and HCT116_Chr3 Cell Lines

For genotyping, sixty six single colonies in total were analyzed by both PCR and RFLP. Twenty six out of sixty six single colonies belonged to transfected HCT116 cell line and forty out of sixty six single colonies belonged to the transfected HCT116_Chr3

cell line. In this section, white arrows in all of the agarose gel electrophoresis figures indicate the single colonies selected for Western blot analysis (Figures 4.5-4.10).

As a result of RFLP (Figure 4.5), single colonies from HCT116-Crispr#6-Col.7 (lanes 3 and 4), HCT116-Crispr#6-Col.19 (lanes 9 and 10), and HCT116-Crispr#6-Col.27cell lines (lanes 13 and 14) were selected for Western blot analysis. There is an approximately 100 bp insertion in HCT116-Crispr#6-Col.7 cell line (lanes 3 and 4). The uncut and cut bands of HCT116-Crispr#6-Col.19 cell line have the same size which shows that the recognition site of the HpyCH4III enzyme is destroyed and DNA cannot be digested by HpyCH4III. The situation for HCT116-Crispr#6-Col.27 cell line is same with HCT116-Crispr#6-Col.19 cell line.

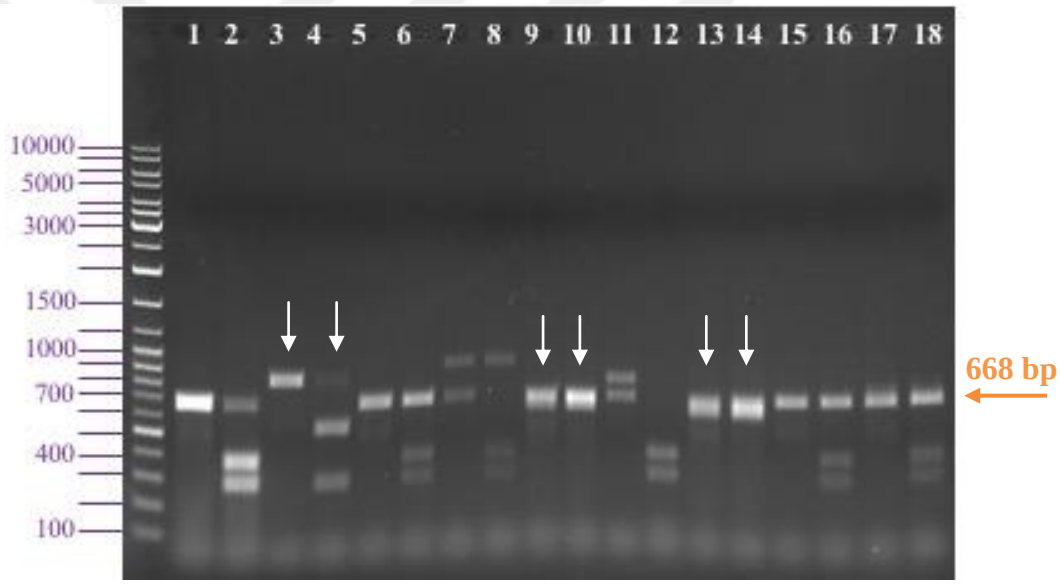

Figure 4.5. Agarose gel electrophoresis analysis of RFLP of amplified PCR products by using total DNAs isolated from Crispr#6 transfected single colonies as a template. Lane 1, HCT116-Puro-Uncut; lane 2, HCT116-Puro-Cut; lane 3, HCT116-Crispr#6-Col.7-Uncut; lane 4, HCT116-Crispr#6-Col.7-Cut; lane 5, HCT116-Crispr#6-Col.12-Uncut; lane 6, HCT116-Crispr#6-Col.12-Cut; lane 7, HCT116-Crispr#6-Col.18-Uncut; lane 8, HCT116-Crispr#6-Col.18-Cut; lane 9, HCT116-Crispr#6-Col.19-Uncut; lane 10, HCT116-Crispr#6-Col.19-Cut; lane 11, HCT116-Crispr#6-Col.21-Uncut; lane 12, HCT116-Crispr#6-Col.21-Cut; lane 13, HCT116-Crispr#6-Col.27-Uncut; lane 14, HCT116-Crispr#6-Col.27-Cut; lane 15, HCT116-Crispr#6-Col.30-Uncut; lane 16, HCT116-Crispr#6-Col.30-Cut; lane 17, HCT116-Crispr#6-Col.31-Uncut; lane 18, HCT116-Crispr#6-Col.31-Cut

RFLP products of HCT116-Crispr#1-Col.25 cell line in Figure 4.6 (lanes 9 and 10). From the evaluation of agarose gel electrophoresis result, it is clearly seen that the uncut band of the HCT116-Crispr#1-Col.25 cell line has the size of 668 bp. The feature of the cut band of that cell line is same as its uncut band. Therefore, the recognition site of HpyCH4III enzyme is destroyed due to the mutation created.

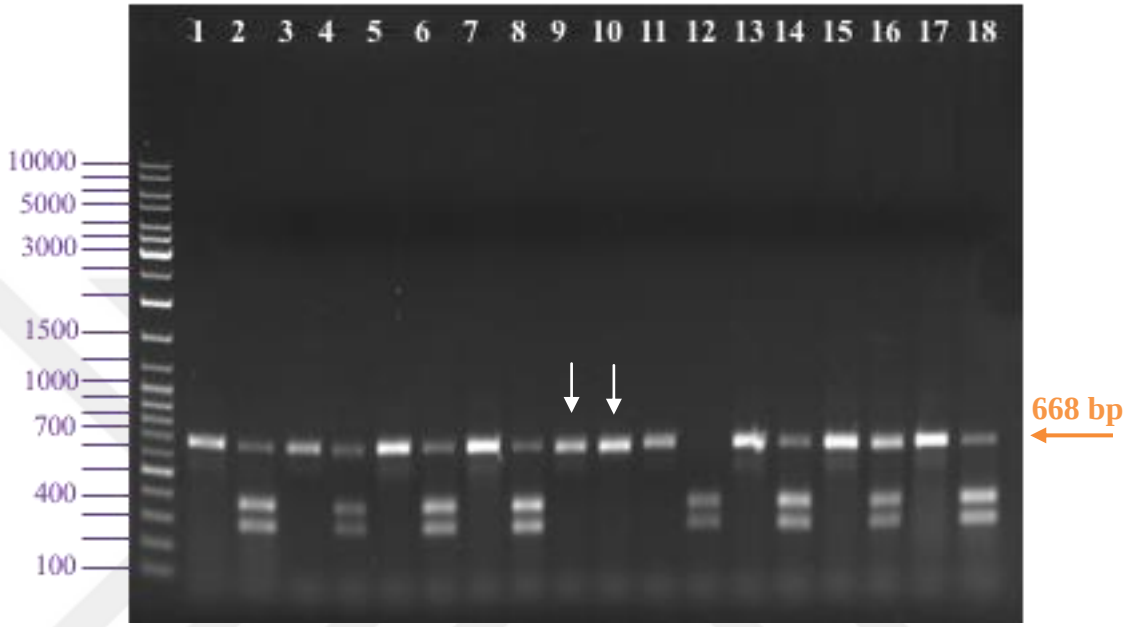

Figure 4.6. Agarose gel electrophoresis analysis of RFLP of amplified PCR products by using total DNAs isolated from Crispr#1 transfected single colonies as a template. Lane 1, HCT116-Puro-Uncut; lane 2, HCT116-Puro-Cut; lane 3, HCT116-Crispr#1-Col.19-Uncut; lane 4, HCT116-Crispr#1-Col.19-Cut; lane 5, HCT116-Crispr#1-Col.22-Uncut; lane 6, HCT116-Crispr#1-Col.22-Cut; lane 7, HCT116-Crispr#1-Col.23-Uncut; lane 8, HCT116-Crispr#1-Col.23-Cut; lane 9, HCT116-Crispr#1-Col.25-Uncut; lane 10, HCT116-Crispr#1-Col.25-Cut; lane 11, HCT116-Crispr#1-Col.31-Uncut; lane 12, HCT116-Crispr#1-Col.31-Cut; lane 13, HCT116-Crispr#1-Col.32-Uncut; lane 14, HCT116-Crispr#1-Col.32-Cut; lane 15, HCT116-Crispr#1-Col.37-Uncut; lane 16, HCT116-Crispr#1-Col.37-Cut; lane 17, HCT116-Crispr#1-Col.39-Uncut; lane 18, HCT116-Crispr#1-Col.39-Cut

RFLP products of HCT116-Crispr#1 and HCT116-Crispr#6 (Figure 4.7) are shown in lanes 3, 4, 5, 6, 7, 8, 11 and 12 named as HCT116-Crispr#6-Col.44, HCT116-Crispr#6-Col.43, HCT116-Crispr#6-Col.45, and HCT116-Crispr#1-Col.12, respectively. The uncut and cut bands of HCT116-Crispr#6-Col.44 cell line indicate that there is a deletion in one allele since the band size is smaller than expected. The cut and uncut band of both HCT116-Crispr#6-Col.43 and HCT116-Crispr#6-Col.45 cell lines are same indicating the disruption of recognition site of HpyCH4III restriction enzyme. The bands of HCT116-Crispr#1-Col.12 indicate that there is an insertion in one allele since there are larger bands above the desired bands.

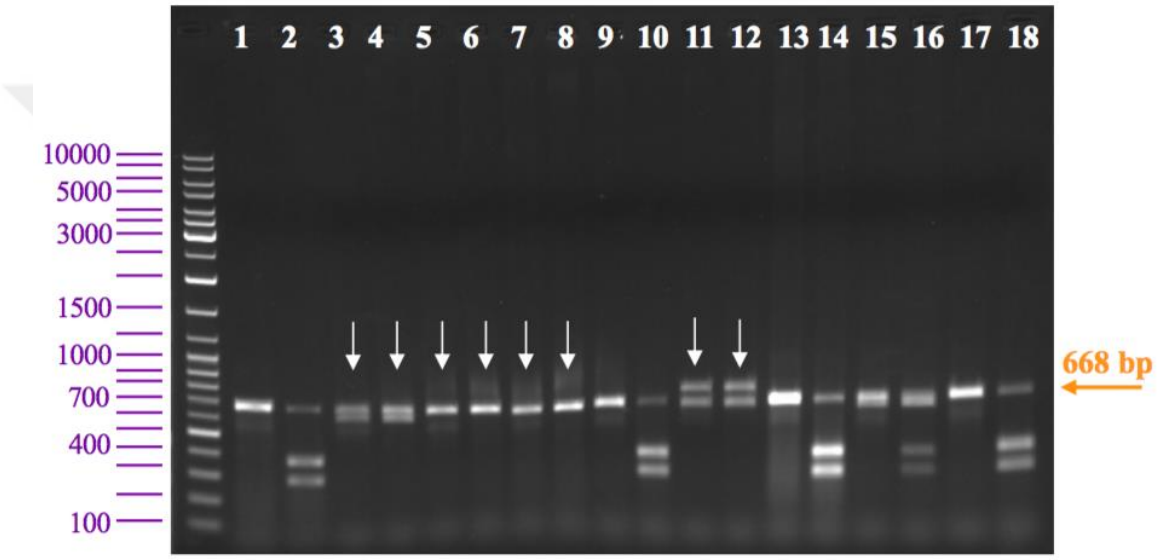

Figure 4.7. Agarose gel electrophoresis analysis of RFLP of amplified PCR products by using total DNAs isolated from Crispr#1 or Crispr#6 transfected single colonies as a template. Lane 1, HCT116-Puro-Uncut; lane 2, HCT116-Puro-Cut; lane 3, HCT116-Crispr#6-Col.44-Uncut; lane 4, HCT116-Crispr#6-Col.44-Cut; lane 5, HCT116-Crispr#6-Col.43-Uncut; lane 6, HCT116-Crispr#6-Col.43-Cut; lane 7, HCT116-Crispr#6-Col.45-Uncut; lane 8, HCT116-Crispr#6-Col.45-Cut; lane 9, HCT116-Crispr#1-Col.6-Uncut; lane 10, HCT116-Crispr#1-Col.6-Cut; lane 11, HCT116-Crispr#1-Col.12-Uncut; lane 12, HCT116-Crispr#1-Col.12-Cut; lane 13, HCT116-Crispr#1-Col.13-Uncut; lane 14, HCT116-Crispr#1-Col.13-Cut; lane 15, HCT116-Crispr#1-Col.14-Uncut; lane 16, HCT116-Crispr#1-Col.14-Cut; lane 17, HCT116-Crispr#1-Col.18-Uncut; lane 18, HCT116-Crispr#1-Col.18-Cut

RFLP products of HCT116_Chr3-Crispr#1-Col.11 cell line are shown in Figure 4.8 (lanes 7 and 8). The uncut band of HCT116_Chr3-Crispr#1-Col.11 cell line suggests that there is an approximately 300 bp insertion.

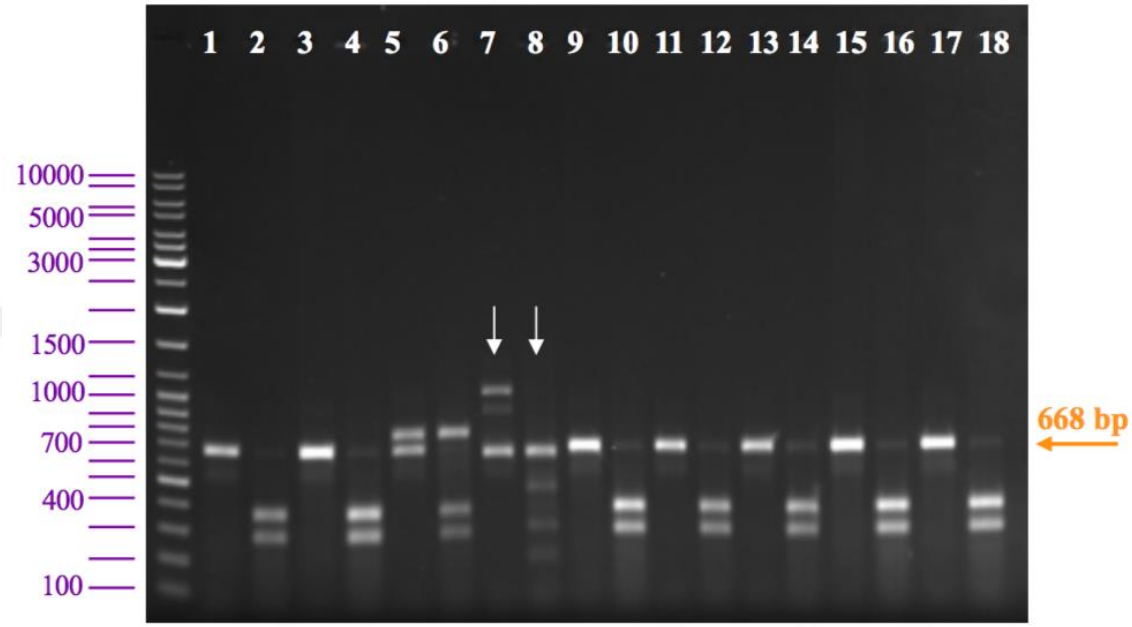

Figure 4.8. Agarose gel electrophoresis analysis of RFLP of amplified PCR products by using total DNAs isolated from Crispr#1 transfected single colonies as a template. Lane 1, HCT116_Chr3-Puro-Uncut; lane 2, HCT116_Chr3-Puro-Cut; lane 3, HCT116_Chr3-Crispr#1-Col.3-Uncut; lane 4, HCT116_Chr3-Crispr#1-Col.3-Cut; lane 5, HCT116_Chr3-Crispr#1-Col.10-Uncut; lane 6, HCT116_Chr3-Crispr#1-Col.10-Cut; lane 7, HCT116_Chr3-Crispr#1-Col.11-Uncut; lane 8, HCT116_Chr3-Crispr#1-Col.11-Cut; lane 9, HCT116_Chr3-Crispr#1-Col.13-Uncut; lane 10, HCT116_Chr3-Crispr#1-Col.13-Cut; lane 11, HCT116_Chr3-Crispr#1-Col.15-Uncut; lane 12, HCT116_Chr3-Crispr#1-Col.15-Cut; lane 13, HCT116_Chr3-Crispr#1-Col.16-Uncut; lane 14, HCT116_Chr3-Crispr#1-Col.16-Cut; lane 15, HCT116_Chr3-Crispr#1-Col.21-Uncut; lane 16, HCT116_Chr3-Crispr#1-Col.21-Cut; lane 17, HCT116_Chr3-Crispr#1-Col.26-Uncut; lane 18, HCT116_Chr3-Crispr#1-Col.26-Cut

Figure 4.9 includes RFLP products of HCT116_Chr3-Crispr#6-Col.11, and HCT116_Chr3-Crispr#6-Col.13 cell lines. Lanes 11 and 12 stands for HCT116_Chr3-Crispr#6-Col.11 cell line and lanes 13 and 14 stands for HCT116_Chr3-Crispr#6-Col.13 cell line. The uncut band of HCT116_Chr3-Crispr#6-Col.11 cell line has a higher position than the expected position which indicates there is an insertion mutation. The bands of HCT116_Chr3-Crispr#6-Col.13 cell line suggest that the recognition site of the HpyCH4III restriction enzyme is disrupted due the mutation created.

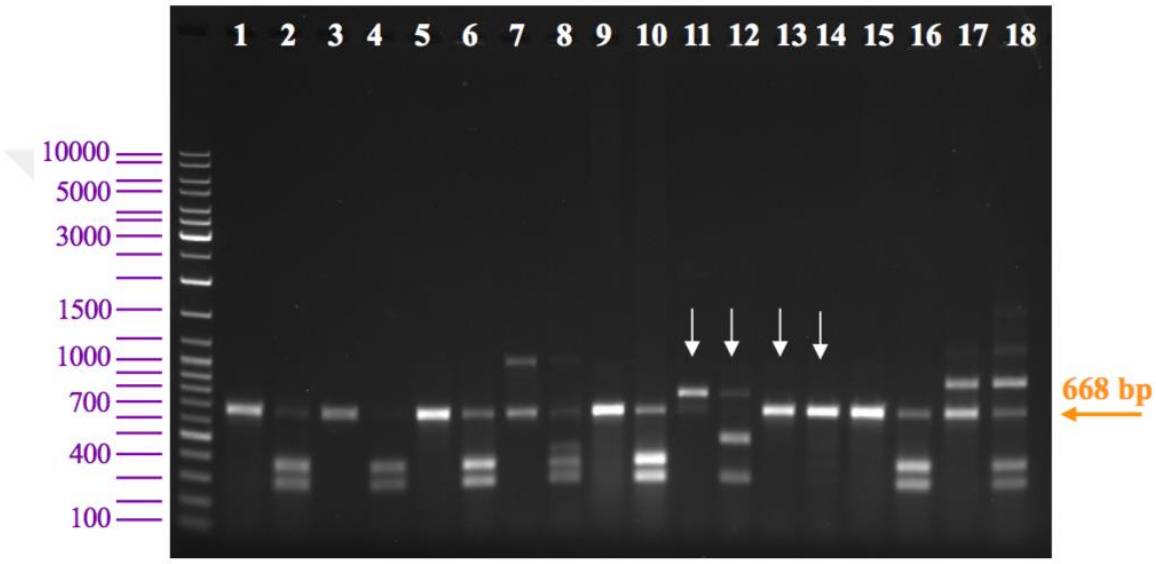

Figure 4.9. Agarose gel electrophoresis analysis of RFLP of amplified PCR products by using total DNAs isolated from Crispr#6 transfected single colonies as a template. Lane 1, HCT116_Chr3-Puro-Uncut; lane 2, HCT116_Chr3-Puro-Cut; lane 3, HCT116_Chr3-Crispr#6-Col.6-Uncut; lane 4, HCT116_Chr3-Crispr#6-Col.6-Cut; lane 5, HCT116_Chr3-Crispr#6-Col.7-Uncut; lane 6, HCT116_Chr3-Crispr#6-Col.7-Cut; lane 7, HCT116_Chr3-Crispr#6-Col.9-Uncut; lane 8, HCT116_Chr3-Crispr#6-Col.9-Cut; lane 9, HCT116_Chr3-Crispr#6-Col.10-Uncut; lane 10, HCT116_Chr3-Crispr#6-Col.10-Cut; lane 11, HCT116_Chr3-Crispr#6-Col.11-Uncut; lane 12, HCT116_Chr3-Crispr#6-Col.11-Cut; lane 13, HCT116_Chr3-Crispr#6-Col.13-Uncut; lane 14, HCT116_Chr3-Crispr#6-Col.13-Cut; lane 15, HCT116_Chr3-Crispr#6-Col.14-Uncut; lane 16,HCT116_Chr3-Crispr#6-Col.14-Cut; lane 17, HCT116_Chr3-Crispr#6-Col.21-Uncut; lane 18, HCT116_Chr3-Crispr#6-Col.21-Cut

RFLP products of HCT116_Chr3-Crispr#1 and HCT116_Chr3-Crispr#6 (Figure 4.10) were shown in well 9, 10, 11, 12, 13, 14, 15, and 16 named as HCT116_Chr3-Crispr#6-Col.24, HCT116_Chr3-Crispr#6-Col.27, HCT116_Chr3-Crispr#6-Col.29 and HCT116_Chr3-Crispr#6-Col.31, respectively. There is an additional larger band in uncut band of HCT116_Chr3-Crispr#6-Col.27, which indicates the insertion mutation. The situation for HCT116_Chr3-Crispr#6-Col.29 and HCT116_Chr3-Crispr#6-Col.31 cell lines are same with each other since both cell lines have same size of bands for both uncut and cut bands. The recognition site of HpyCH4III restriction enzyme is destroyed because the sizes of cut bands of these cell lines are as same as the uncut bands.

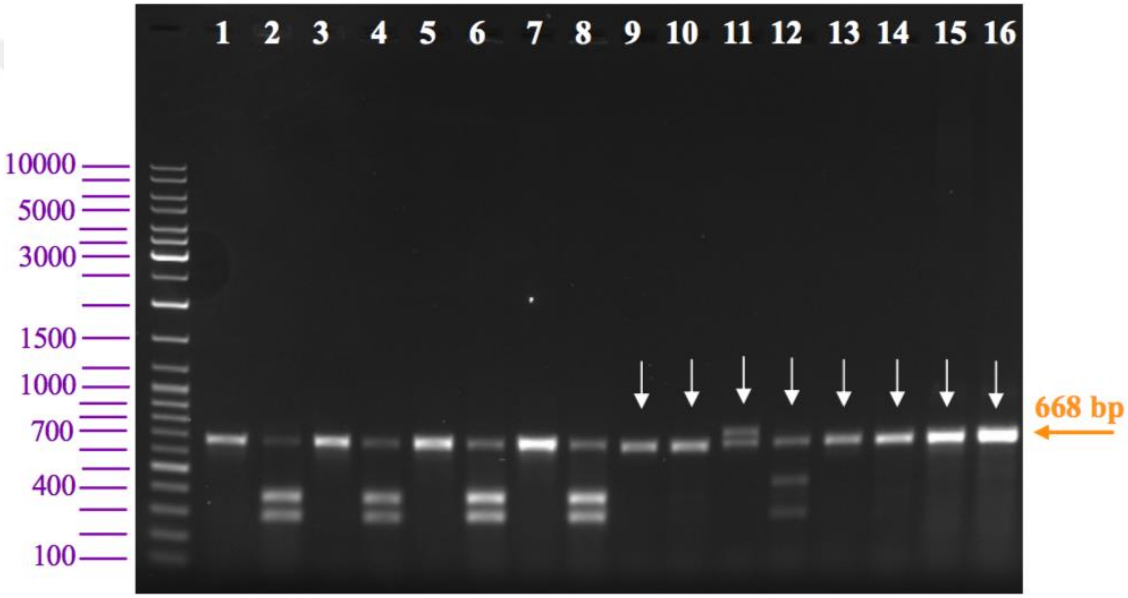

Figure 4.10. Agarose gel electrophoresis analysis of RFLP of amplified PCR products by using total DNAs isolated from Crispr#1 or Crispr#6 transfected single colonies as a template. Lane 1, HCT116_Chr3-Puro-Uncut; lane 2, HCT116_Chr3-Puro-Cut; lane 3, HCT116_Chr3-Crispr#1-Col.23-Uncut; lane 4, HCT116_Chr3-Crispr#1-Col.23-Cut; lane 5, HCT116_Chr3-Crispr#1-Col.24-Uncut; lane 6, HCT116_Chr3-Crispr#1-Col.24-Cut; lane 7, HCT116_Chr3-Crispr#1-Col.27-Uncut; lane 8, HCT116_ HCT116_Chr3-Crispr#1-Col.27-Cut; lane 9, HCT116_Chr3-Crispr#6-Col.24-Uncut; lane 10, HCT116_Chr3-Crispr#6-Col.24-Cut; lane 11, HCT116_Chr3-Crispr#6-Col.27-Uncut; lane 12, HCT116_Chr3-Crispr#6-Col.27-Cut; lane 13, HCT116_Chr3-Crispr#6-Col.29-Uncut; lane 14, HCT116_Chr3-Crispr#6-Col.29-Cut; lane 15, HCT116_Chr3-Crispr#6-Col.31-Uncut; lane 16, HCT116_Chr3-Crispr#6-Col.31-Cut

4.5. Western Blot Analysis of Chosen Colonies

Colonies that have the biallelic mutations were chosen from the RFLP analysis used for Western Blot analysis. The chosen colonies were listed in Table 4.1. All of the colonies listed in Table 4.1 were grown under cell culture conditions and used for cell extract preparation. Unfortunately, single colonies of HCT116-Crispr#6-Col.7 and HCT116_Chr3-Crispr#6-Col.24 cell lines were eliminated because of their inefficient growth.

Table 4.1. Single colonies chosen for Western Blot analysis

HCT116	HCT116_Chr3
Crispr#1 → 12, 25	**Crispr#1 →** 11
Crispr#6 → 7, 19, 27, 43, 44, 45	**Crispr#6 →** 8, 11, 13, 17, 24, 27, 29, 31

The equal amount of protein from the cell extracts was used for Western blot analysis (Figure 4.11 and Figure 4.12). The percentage of knockdown efficiency was determined by the quantitative analysis of density of the bands using ImageLab (Table 4.2). Moreover, the quantitative analysis of Western blot data is summarized graphically in Figure 4.14 in order to provide a comparison between percentages of knockdown efficiencies and densities of the samples.

The quantitative analysis of Western blot showed that some of the single cell colonies have valuable knockdown efficiencies. In general, the knockdown efficiencies of single colonies of HCT116 are more successful than single colonies of HCT116_Chr3.

The knockdown efficiency of polγ of HCT116-Crispr#6-Col.43 cell line is 99.16% which is the highest percentage of knockdown (Figure 4.12; lane 4). The polγ of HCT116-Crispr#1-Col.12 cell line has 95.56% knockdown efficiency (Figure 4.12; lane 2). The knockdown percentage of polγ of HCT116-Crispr#6-Col.44 is 93.31% (Figure 4.12; lane 5). Polγ of HCT116-Crispr#6-Col.27 cell line is 60.41% knocked down (Figure 4.11; lane 4). Although polγ of HCT116-Crispr#6-Col.27 cell line seems like knocked down qualitatively, it was not included into sequencing analysis because its low knockdown percentage.

Generally, the knockdown efficiency of single colonies of HCT116_Chr3 cell line is low. HCT116_Chr3-Crispr#6-Col.27 cell line has the highest polγ knockdown percentage among the other single colonies of HCT116_Chr3 cell line (Figure 4.12;

lane 10) and polγ of this cell line is 85.10% knocked down. HCT116_Chr3-Crispr#1-Col.11 HCT116_Chr3-Crispr#6-Col.11 cell lines were also selected for Western blot analysis and their knockdown efficiency percentages are 28.24% and 32.71%, respectively.

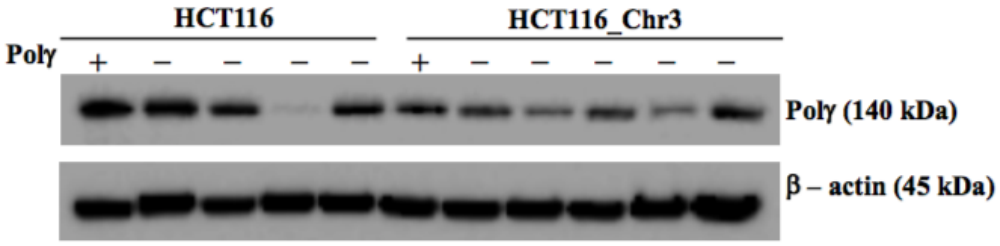

Figure 4.11. Western Blot analysis performed with chosen single colonies. Lane 1, HCT116-wt; lane 2, HCT116-Crispr#6-Col.19; lane 3, HCT116-Crispr#1-Col.25; lane 4, HCT116-Crispr#6-Col.27; lane 5, HCT116-Crispr#6-Col.45; lane 6, HCT116_Chr3-wt; lane 7, HCT116_Chr3-Crispr#6-Col.8; lane 8, HCT116_Chr3-Crispr#1-Col.11; lane 9, HCT116_Chr3-Crispr#6-Col.13; lane 10, HCT116_Chr3-Crispr#6-Col.27; lane 11, HCT116_Chr3-Crispr#6-Col.31

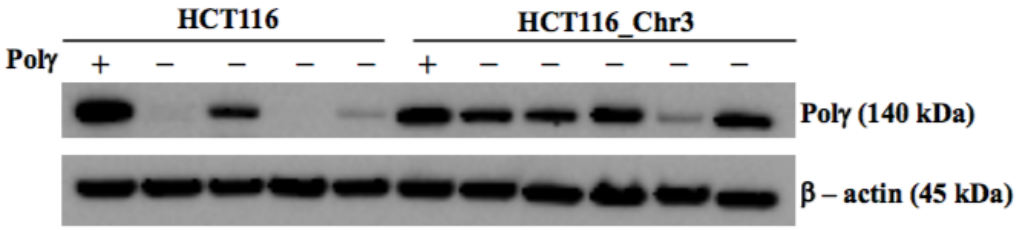

Figure 4.12. Western Blot analysis performed with of chosen single colonies. Lane 1, HCT116-wt; lane 2, HCT116-Crispr#1-Col.12; lane 3, HCT116-Crispr#6-Col.27; lane 4, HCT116-Crispr#6-Col.43; lane 5, HCT116-Crispr#6-Col.44; lane 6, HCT116_Chr3-wt; lane 7, HCT116_Chr3-Crispr#1-Col.11; lane 8, HCT116_Chr3-Crispr#6-Col.11; lane 9, HCT116_Chr3-Crispr#6-Col.17; lane 10, HCT116_Chr3-Crispr#6-Col.27; lane 11, HCT116_Chr3-Crispr#6-Col.29

Table 4.2. Quantification data of Western Blot analysis

Samples	Knockdown %	(Polγ/HCT116)*100	Polγ - 140 kDa	β-actin – 45 kDa	Polγ / β-actin
HCT116-wt			2092728 or 4209725	2641661 and 3381975	0,792201573 and 1,24475343549257
HCT116-Crispr#1-Col.12	95.56	4,44	186876	3619448	0,051631077
HCT116-Crispr#1-Col.25	36.24	63,76	1334270	2249247	0,593207416
HCT116-Crispr#6-Col.19	4.95	95,05	1989144	3093708	0,642964365
HCT116-Crispr#6-Col.27	60.41	39,59	1666561	2733393	0,60970413
HCT116-Crispr#6-Col.43	99.16	0,84	35544	3700802	0,009604405
HCT116-Crispr#6-Col.44	93.31	6,69	281808	3294228	0,085545991
HCT116-Crispr#6-Col.45	36.01	63,99	1339140	2599938	0,515066128
Samples	**Knockdown %**	**(Polγ/HCT116_Chr3)*100**	**Polγ - 140 kDa**	**β-actin – 45 kDa**	**Polγ / β-actin**
HCT116_Chr3-wt			3113539 or 1172567	3263928 or 2644257	0,953923922 or 0,443439121083919
HCT116_Chr3-Crispr#1-Col.11	28.24	71.76	2234196	3239158	0,689745915
HCT116_Chr3-Crispr#6-Col.8	13.34	86.66	1016090	2673077	0,380119989
HCT116_Chr3-Crispr#6-Col.11	32.71	67.29	2095164	3830820	0,546923113
HCT116_Chr3-Crispr#6-Col.13	17.45	82.55	967950	2646501	0,365747075
HCT116_Chr3-Crispr#6-Col.17	16.47	83.53	2600754	4028808	0,645539326
HCT116_Chr3-Crispr#6-Col.27	85.10	14.90	464016	3312868	0,140064741
HCT116_Chr3-Crispr#6-Col.29	16.98	83.02	2584862	3431106	0,753361161
HCT116_Chr3-Crispr#6-Col.31	-19.69	119.69	1403424	4301094	0,326294659

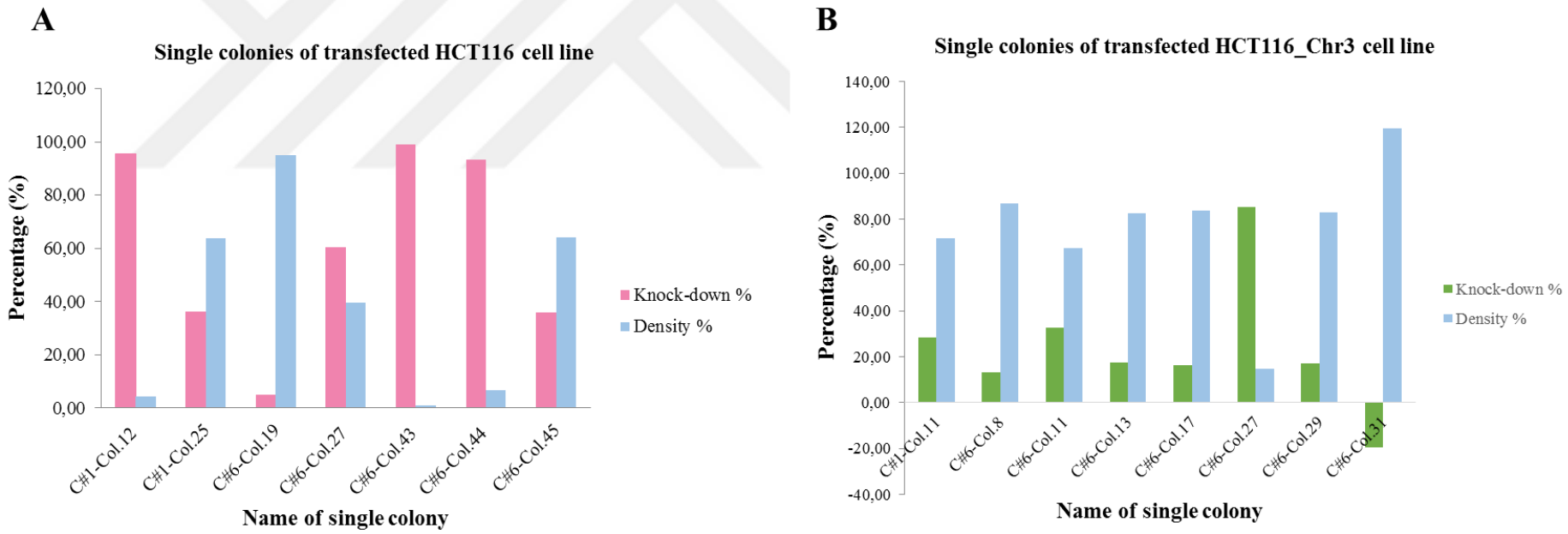

Figure 4.13. Knockdown and density percentage (%) graph of single colonies of transfected HCT116 and HCT116_Chr3 cell lines.

Consequently, six colonies out of fifteen colonies were chosen for the further analysis. In order to check the consistency of these colonies, PCR of colonies chosen from the Western blot analysis performed and run on a agarose gel electrophoresis as shown in Figure 4.14. The first well after the ladder is the positive control (mock) named as HCT116-Puro and the rest are HCT116-Crispr#1-Col.12, HCT116-Crispr#6-Col.43, HCT116-Crispr#6-Col.44, HCT116_Chr3-Crispr#1-Col.11, HCT116_Chr3-Crispr#6-Col.11, and HCT116_Chr3-Crispr#6-Col.27.

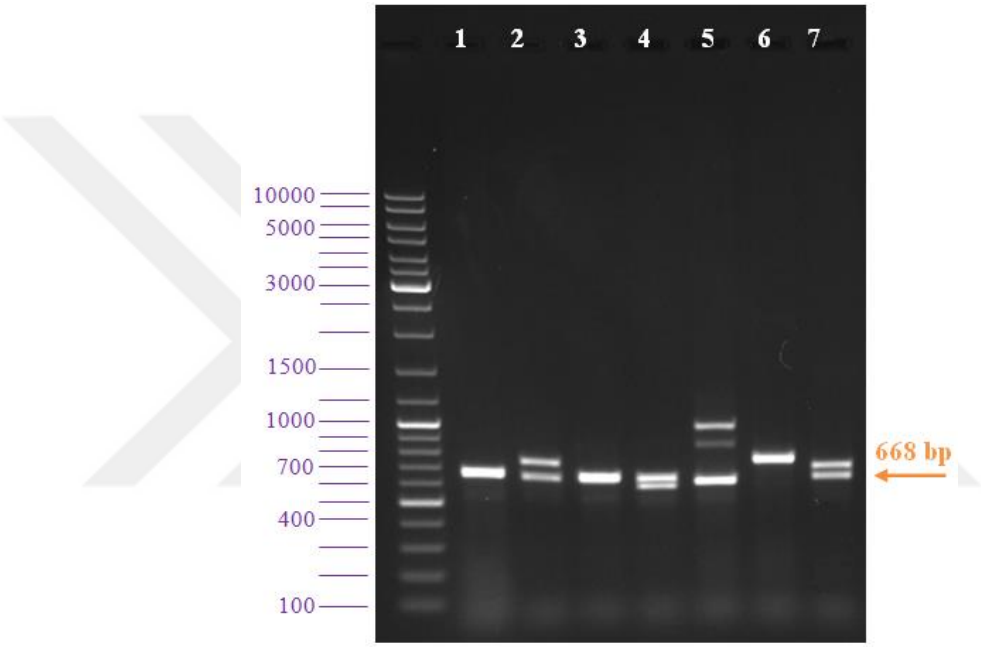

Figure 4.14. Agarose gel electrophoresis analysis of amplified PCR products by using total DNAs isolated from chosen single colonies as a template. Lane 1, HCT116-Puro; lane 2, HCT116-Crispr#1-Col.12; lane 3, HCT116-Crispr#6-Col.43; lane 4, HCT116-Crispr#6-Col.44; lane 5, HCT116_Chr3-Crispr#1-Col.11; lane 6, HCT116_Chr3-Crispr#6-Col.11; lane 7, HCT116_Chr3-Crispr#6-Col.27

4.6. Transformation of TA Cloning Products

The DNA from the ligation reaction (Section 3.4.8; Table 3.16) was transformed into the competent bacteria. Then, the transformation efficiency was checked by culturing the transformation reaction onto an agar plate w/amp. In Figure 4.15, culturing of transformed DNA samples to competent bacteria is shown. Because agar plates were only mixed with ampicillin, enough information cannot be obtained for selecting bacterial colony that has the CRISPR plasmid from the plates. In other words, it was very hard to determine whether the selected colony includes the desired insert or not since all of the colonies have the same appearance. That's why blue-white screening was used for more efficient selection.

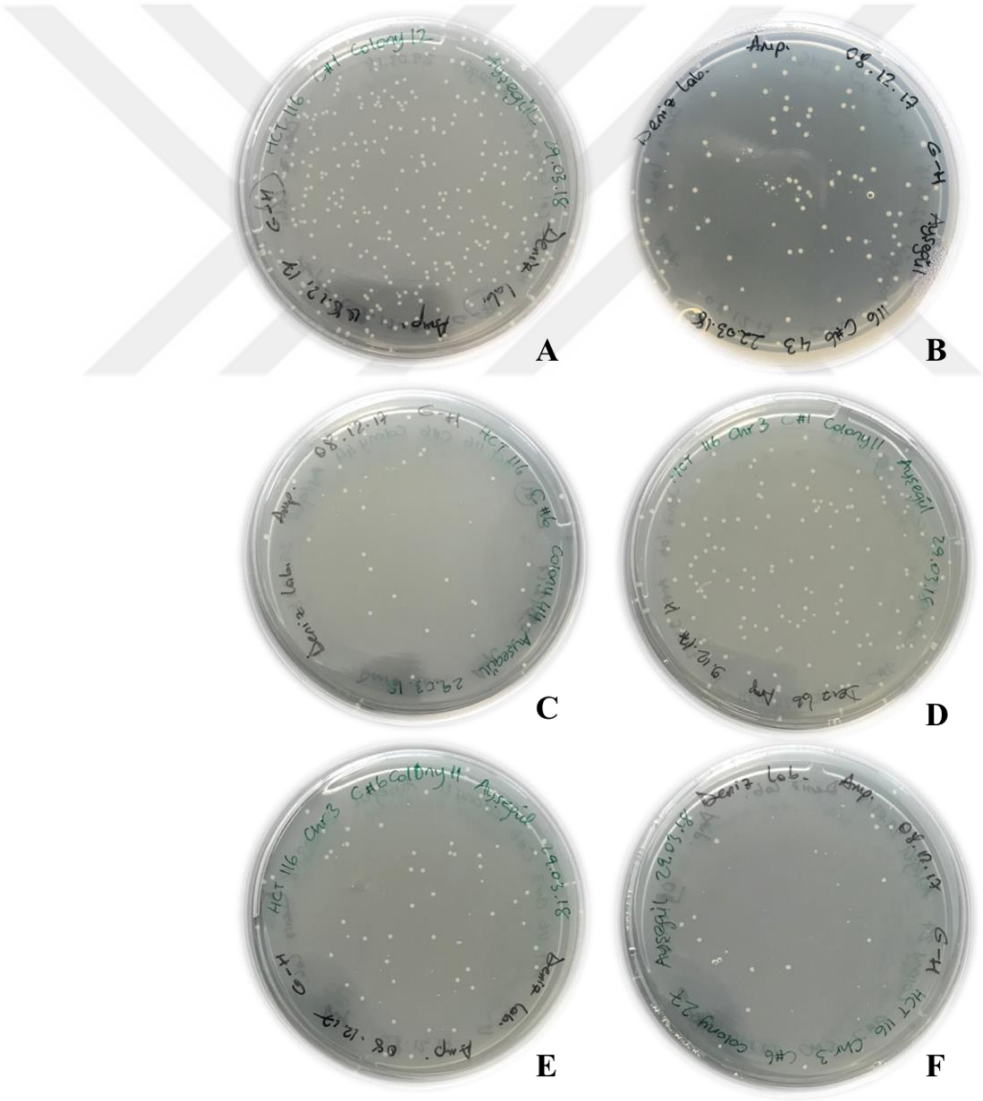

Figure 4.15. Agar plates obtained from transformation: **A.** HCT116-Crispr#1-Col.12, **B.** HCT116-Crispr#6-Col.43, **C.** HCT116-Crispr#6-Col.44, **D.** HCT116_Chr3-Crispr#1-Col.11, **E.** HCT116_Chr3-Crispr#6-Col.11, and **F.** HCT116_Chr3-Crispr #6- Col.27

4.7. Blue-White Screening of Chosen Colonies

In order to provide discrimination between CRISPR plasmids and empty plasmids, agar plates were incubated with X-gal and IPTG in addition to amp. The results of blue-white screening are shown in Figure 4.16. The color difference between the colonies provides information about the insertion of CRISPR into plasmid. The color of the colony could either be white or blue. It is known that white colonies are the colonies that include the insert. On the other hand, blue colonies are the colonies with no insert.

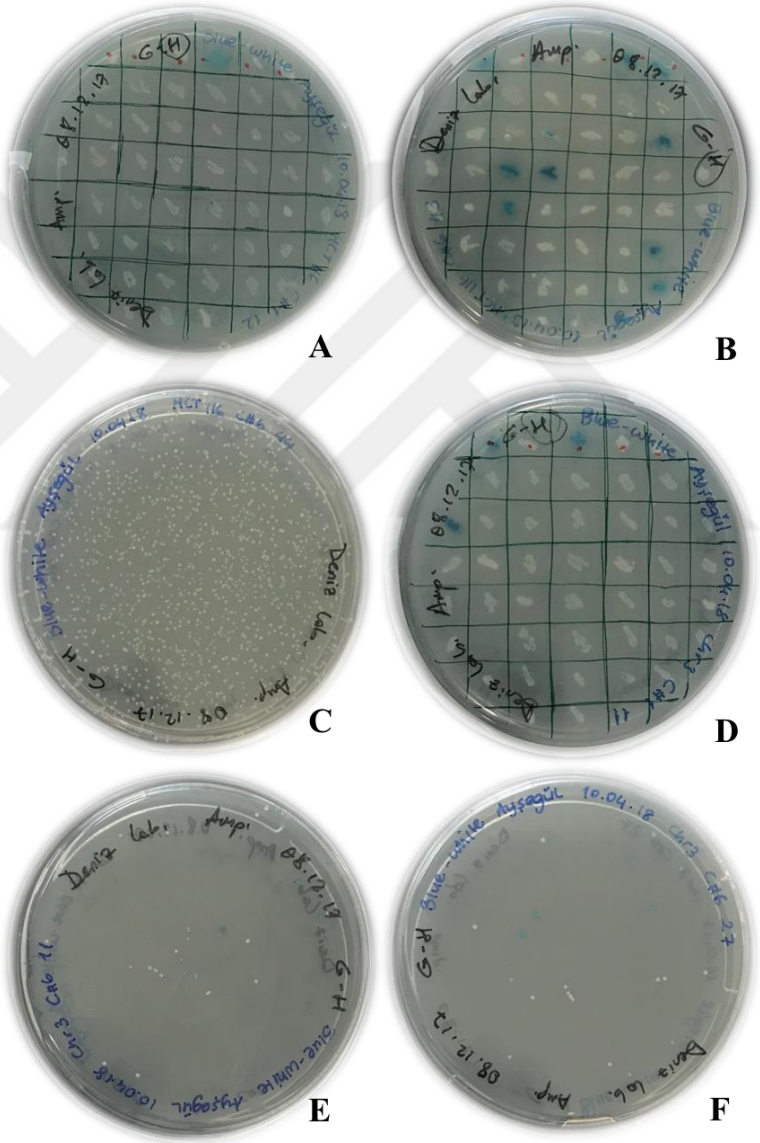

Figure 4.16. Agar plates obtained from blue-white screening: **A.** HCT116-Crispr#1-Col.12, **B.** HCT116-Crispr#6-Col.43, **C.** HCT116-Crispr#6-Col.44, **D.** HCT116_Chr3-Crispr#1-Col.11, **E.** HCT116_Chr3-Crispr#6-Col.11, and **F.** HCT116_Chr3-Crispr#6-Col.27

4.8. Sequencing Data of Isolated Plasmid DNAs

The sequencing data of the plasmid DNAs isolated from the plates of the blue-white screening were obtained from MC Lab, USA. For TA cloning procedure six colonies were chosen from the plates shown in Figure 4.16:

- HCT116-Crispr#1-Col.12,
- HCT116-Crispr#6-Col.43,
- HCT116-Crispr#6-Col.44,
- HCT116_Chr3-Crispr#1-Col.11,
- HCT116_Chr3-Crispr#6-Col.11,
- HCT116_Chr3-Crispr#6-Col.27

From each plate, sixteen plasmid DNAs were isolated and in total 96 plasmid DNAs were sent for Sanger sequencing (Figure 4.17). A color code was used for summarizing the reliable sequencing data of plasmid DNAs. Colorless wells indicate that there is no qualified information about sequencing. Different colors are chosen for plasmid DNAs of different single cell line.

The very first line in the figures of Sanger sequencing analysis (Figures 4.18-4.21) represents the sequence of wild-type (wt) DNA. For the sequence of wt, 66 bp out of 668 bp were chosen since that region includes sequence of start codon, restriction enzyme cut site and targeted designs of both Crispr#1 and Crispr#6.

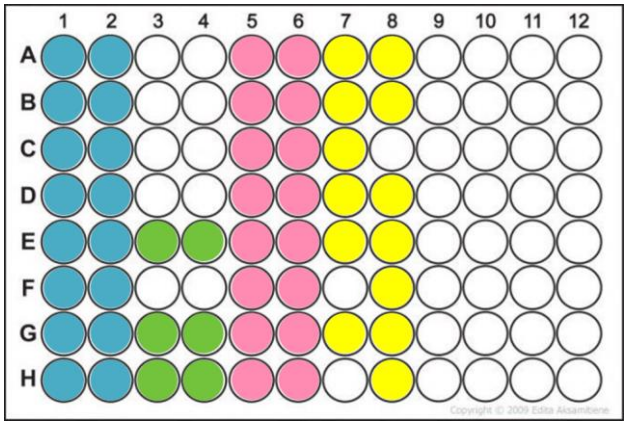

Figure 4.17. A representative image for loading order of plasmid DNAs. Each color indicates different type of cell lines. Colorless wells of the 96-well plate represent the samples that have no informative sequencing data. Blue color stands for HCT116-Crispr#1-Col.12 cell line. Green color stands for HCT116-Crispr#6-Col.43 cell line. Pink color stands for HCT116-Crispr#6-Col.44 cell line. Yellow color stands for HCT116_Chr3-Crispr#1-Col.11.

Unfortunately, sequencing data analysis could not be done for the cell lines of HCT116_Chr3-Crispr#6-Col.11 and HCT116_Chr3-Crispr#6-Col.27 because there was no qualified information about the sequences of these samples. Thus, the DNA sequencing was not performed properly.

Fourteen out of sixteen samples of HCT116-Crispr#1-Col.12 cell line provided valuable information. Ten of the samples has deletion mutation and it is found that 10 bp were deleted in compared to sequence of wt. The rest of the samples of HCT116-Crispr#1-Col.12 cell line has insertion mutation and there were 87 bp inserted (=) through the restriction enzyme cut site (Figure 4.18).

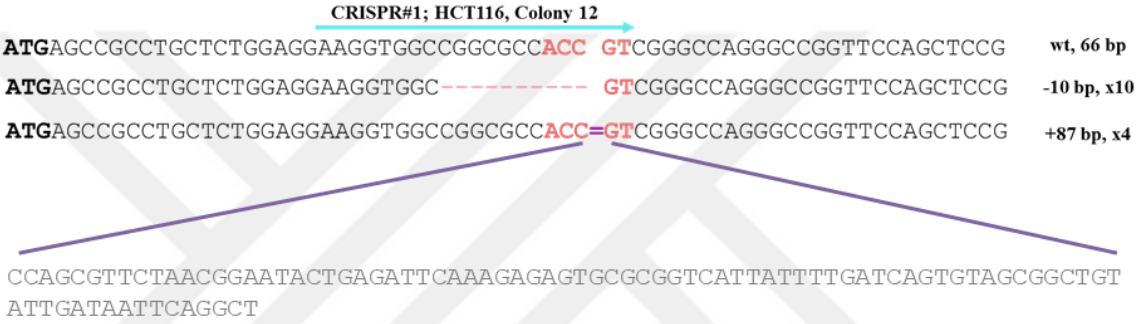

Figure 4.18. Sanger sequencing analysis of HCT116-Crispr#1-Col.12 cell line. The binding site (20 nt) of Crispr#1 (blue arrow), and restriction enzyme (HpyCH4III) cut site (coral) are shown in the figure. The mutations are represented according to its type: dashed line (pink), and equity sign (purple) indicates deletion and insertion mutations, respectively.

Four of the plasmid DNAs of HCT116-Crispr#6-Col.43 cell line (Figure 4.19) gave information for sequencing analysis. Unfortunately, the trace data obtained from the others are not reliable. The analysis showed that there is deletion of 2 bp and 1 bp in three and one of the samples, respectively.

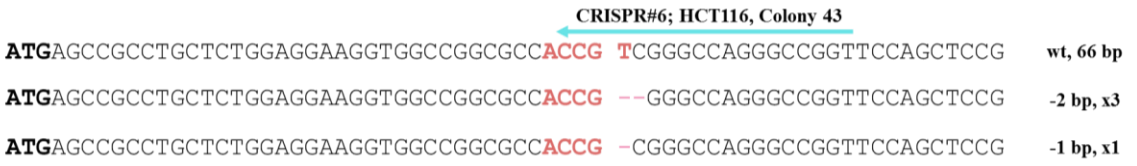

Figure 4.19. Sanger sequencing analysis of HCT116-Crispr#6-Col.43 cell line. The binding site (20 nucleotides) of CRISPR#6 (blue arrow), restriction enzyme (HpyCH4III) cut site (coral) are shown in the figure. The mutations were represented according to its type: dashed line (pink) indicates deletion mutation.

Eleven samples gave a valuable information about the plasmid DNAs obtained from the cell line of HCT116-Crispr#6-Col.44 (Figure 4.20). Fifty five bp are deleted from five out of eleven samples. In one of the sample 1 bp entered in between the nucleotides of restriction enzyme cut site.

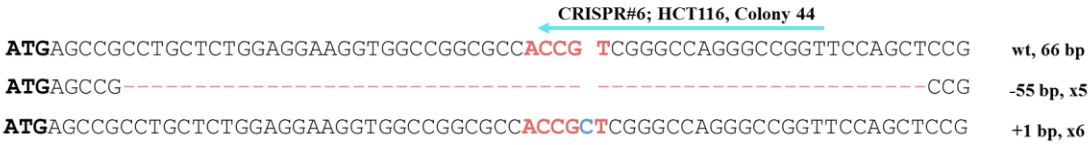

Figure 4.20. Sanger sequencing analysis of HCT116-Crispr#6-Col.44 cell line. The binding site (20 nt) of Crispr#6 (blue arrow), restriction enzyme (HpyCH4III) cut site (coral) are shown in the figure. The mutations are represented according to its type: dashed line (pink), and different colored nucleotide (blue) indicate deletion and transversion mutations, respectively.

The final cell line that had reliable sequencing data was HCT116_Chr3-Crispr#1-Col.11. From ten out of twelve samples 27 bp were deleted and 378 bp (=) are inserted into two of the samples (Figure 4.21).

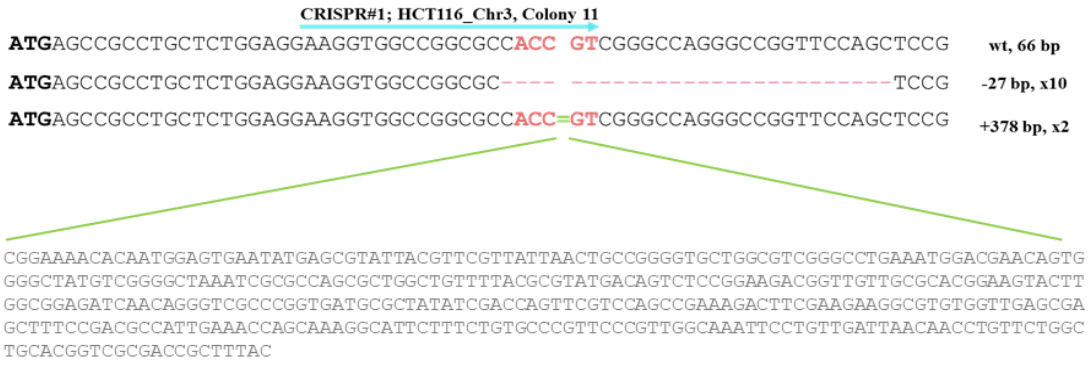

Figure 4.21. Sanger sequencing analysis of HCT116_Chr3-Crispr#1-Col.11 cell line. The binding site (20 nt) of Crispr#1 (blue arrow), restriction enzyme (HpyCH4III) cut site (coral) are shown in the figure. The mutations were represented according to its type: dashed line (pink), and equity sign (purple) indicate deletion and insertion mutations respectively.

5. DISCUSSION AND CONCLUSION

DNA is damaged due to endogenous or exogenous agents. Cells have DNA repair mechanisms for getting rid of DNA damages. The major DNA repair mechanism for oxidative, alkylating and deaminated DNA lesions and SSBs is BER. This repair mechanism is involved in both nucleus and mitochondria. The working principle of the BER pathway of nucleus is similar to that of mitochondria. In nuclear BER, the polymerase activity is provided by polβ whereas polγ takes place in mtBER. Thus, polγ found in mitochondria plays a crucial role in mtBER and also in the replication of mtDNA.

The synthetic lethality between polγ and MLH1 is an important approach to kill MLH1 mutated/deficient cancer cells selectively through the small molecule inhibitors of polγ. This is an advantageous way of selective tumor cell death since the healthy cells are not disrupted by the occurrence of synthetic lethality. The tumor suppressor protein MLH1 plays a role in MMR. Besides its repair function during DNA replication, MMR also involves in the repair of oxidative DNA damage and thus it is a backup mechanism of BER. Thus, polγ inhibition is a powerful target for the selective treatment of MLH1 deficient nonpolyposis colon cancer (HCT116 cell lines). To determine if polγ inhibitors-mediated tumor or cancer cell death is only through the cellular function of polγ without affecting other cellular processes, polγ knockdown cells are needed. For this purpose, the catalytic subunit of the polγ protein was targeted by using CRISPR/Cas9 technology.

In this study, the effects of two different 20 nucleotides long single guide RNA (sgRNA; Crisrpr#1 or Crispr#6) on HCT116 and HCT116_Chr3 cell lines were examined. First of all, the first exon of the catalytic subunit of polγ was targeted for the *polγ* gene silencing, because it has all the enzymatic activities. The catalytic subunit of polγ designed according to CRISPR/Cas9 technology was cloned into Puro plasmid. Then, isolated plasmid DNAs containing the targeted sequences (Crispr#1 or Crispr#6) in the Puro plasmid were introduced into HCT116 and HCT116_Chr3 cell lines by PEI transfection. The growth rate of transfected HCT116 and HCT116_Chr3 cell lines was slower than wt cell lines. In order to provide the cell survival, sodium pyruvate and

uridine were added into the cell culture mediums of transfected cells as additional compounds. Pyruvate is a hydrogen receptor which produces NAD from NADH. Uridine plays role in biosynthesis of pyrimidine in mitochondria which supports the mtDNA replication. Hence, the ATP production in mitochondria was supported in these cell lines [57, 58]. Although growth of cells was supported by additional compounds, the proliferation rate of the cells was significantly slow. In order to surpass this situation the concentration of sodium pyruvate and uridine might be increased. Then, single colonies were obtained using puromycin containing selection medium. For the CRISPR/Cas9 gene targeting efficiency, the basic biotechnological methodologies were used like PCR, RFLP, Western blot analysis and sequencing.

The genotyping analysis of the transfected pools and single colonies were started by amplifying the part surrounding the CRISPR target site in polγ. The expected PCR product size was 668 bp and the PCR product size was verified by agarose gel electrophoresis and then genotyping was performed with RFLP analysis. For RFLP analysis, the PCR product was divided into two. One was not digested with restriction enzyme (called as uncut), and the other one was digested with HpyCH4III restriction enzyme (called as cut). Figure 4.4 shows that digested PCR products of CRISPR/Cas9-mediated mutant clones were uncut, indicating that both Crispr#1 and Crispr#6 were successfully introduced into both transfected pools of HCT116 and HCT116_Chr3 cell lines. The digested mock PCR products (HCT116-Puro and HCT116_Chr3-Puro) were cut as expected (Figure 4.4). Then, these cell lines were used for the selection of single colonies and genotyping analysis of single colonies.

Fifteen different single colony cells that possibly have biallelic mutations were chosen (Table 4.1) for Western blot analysis. The quantitative densitometric analysis of Western blot showed that six of the single cell colonies have valuable knockdown efficiencies. In general, the knockdown efficiencies of single colonies of HCT116 are more successful than single colonies of HCT116_Chr3. For example, the knockdown efficiency of polγ of HCT116-Crispr#6-Col.43 cell line is 99.16% which is the highest percentage of knockdown (Figure 4.12; lane 4). The polγ of HCT116-Crispr#1-Col.12 cell line has 95.56% knockdown efficiency (Figure 4.12; lane 2).

RFLP and Western blot data interpreted simultaneously for TA cloning and sequencing analysis. Accordingly, only 6 of the single colonies out of 15 were

promising. That's why 6 of the single colonies were sequenced. Before the sequencing, PCR products of six single colonies were run on agarose gel electrophoresis and then bands were extracted from the gel. The obtained DNAs were ligated into the plasmid (pTZ57R/T) and then transformed into competent bacteria. The selection of plasmid DNA including the targeted sequence was done by blue-white screening. In this screening, white colonies have the desired plasmid DNAs whereas blue colonies not. Thus, plasmid DNAs of white colonies were isolated by using alkaline lysis method for sequencing analysis.

For each single colony, 16 plasmid DNAs were sequenced. The frame-shift mutations leading to stop codon or a nonsense-mediated decay (NMD) was created on polγ gene by CRISPR/Cas9 technology. When frameshift mutations create a nonsense stop codon, the translation of the protein cannot be completed properly and truncated protein is produced [23]. According to Sanger sequencing analysis, HCT116-Crispr#1-Col.12 cell line has 87 bp insertions in one of polγ allele and there is a 10 bp deletion in its other allele (Figure 4.18). It has been found that the sequence of the insertion belongs to the bacterial genome by using NCBI BLAST and an early stop codon is created due to the insertion. Also, in the other allele of HCT116-Crispr#1-Col.12 cell line there is a 10 bp deletion and a stop codon is created 260 amino acids after the start codon of polγ. The sequencing data analysis of HCT116-Crispr#6-Col.43 (Figure 4.19) cell line indicates that 1-2 bp are deleted and a stop codon is created 242 amino acids after the start codon of polγ. In HCT116-Crispr#6-Col.44 (Figure 4.20) cell line, 55 bp was deleted and a stop codon was seen 246 amino acids after the start codon of polγ. The last cell line that has the sequencing data is named as HCT116_Chr3-Crispr#1-Col.11 (Figure 4.21). In this cell line, 27 bp are deleted which is the multiple of three. That's why the stop codon of polγ appears nine codons before the original stop codon. Thus, the sequencing data analysis showed that three of the chosen single colonies are knocked down.

In conclusion, a frame-shift mutation was created on *polγ* gene by CRISPR/Cas9 technology which caused to the premature stop codon and then polγ gene silencing. Consequently, three of the single cell colonies were identified as polγ knockdown cells. The effect of polγ inhibitors will be studied in the polγ silenced HCT116 and HCT116_Chr3 cell lines.

REFERENCES

1. Reece JB., Urry LA., Cain ML., Wasserman SA., Minorsky PV., Jackson RB., Campbell Biology. 9th edition. USA:Pearson; 2011. p. 156.
2. McCarron J., Wilson C., Sandison M., From Structure to Function: Mitochondrial Morphology, Motion and Shaping in Vascular Smooth Muscle. Journal of Vascular Research. 2013; (50):350-371
3. Kühlbrandt W., Structure and function of mitochondrial membrane protein complexes. BMC Biology. 2015.
4. Smith RAJ., Hartley RC., Cocheme HM., Mitochondrial pharmacology. Cell Press. 2012.
5. Murphy MP., How mitochondria produce reactive oxygen species. Biochem Journal. 2009; 417, 1–13.
6. Bigarella CL., Liang R., Ghaffari S., Stem cells and the impact of ROS signaling. The Company of Biologists Ltd. 2014; 141, 4206-4218.
7. Pecorino L., Molecular Biology of Cancer. 3rd edition. UK:Oxford University Press. 2012; p. 154-157
8. Circu ML., Aw TY., Reactive Oxygen Species, Cellular Redox Systems And Apoptosis. NIH PA. 2010; 48(6): 749–762.
9. Rohan TE., Wong L., Wang T., Haines J., Kabat GC. Do Alterations in Mitochondrial DNA Play a Role in Breast Carcinogenesis?. Journal of Oncology. 2010.
10. Taylor RW., Turnbull DM., Mitochondrial DNA Mutations In Human Disease. Nature. 2015; (6):389-402.
11. McKinney EA., Oliveira MT., Replicating animal mitochondrial DNA. Genetics and Molecular Biology, 2013; 36, 308-315.
12. Saccone C., Gadaleta G., Mitochondrial Genome. Wiley. 2017.
13. Koehler C., Bauer MF, Mitochondrial Function and Biogenesis. Springer. 2004. 181.
14. Vega RB., Horton JL., Kelly DP., Maintaining Ancient Organelles. 2015.
15. Mathews CK, Holde KEV, Appling DR, Cahill SJA, Biochemistry. 4th edition. USA:Pearson. 2013. p. 1041
16. Wood RD. and Doublié S., DNA polymerase θ (POLQ), double-strand break repair, and cancer. 2016. History of the Human Sciences.
17. Apostolova N.,Esplugues JV., Mitochondrial DNA Replication in Health and Disease. Intech. 2011.
18. DNA polymerase gamma, catalytic subunit. National Institute of Health [Online] https://ghr.nlm.nih.gov/gene/POLG#location

19. DNA polymerase gamma 2, accessory subunit. National Institute of Health [Online] https://ghr.nlm.nih.gov/gene/POLG2#location

20. Nurminena A., Farnumb GA., Kagun LS., Pathogenicity in POLG syndromes: DNA polymerase gamma pathogenicity prediction server and database. Elsevier. 2017; 7, 147–156

21. Copeland WC., Defects in Mitochondrial DNA Replication and Human Disease. National Institute of Health PA. 2012; 47(1): 64–74

22. Krasich R., Copeland WC., DNA polymerases in the mitochondria: A critical review of the evidence. History of Health Science. 2017; 22: 692–709.

23. Alberts B, Johnson A, Lewis J, Morgan D, Raff M, Roberts K, Walter P., Molecular Biology of the Cell. 6th edition. USA:Garland Science. 2015; p. 352-353, 661

24. Gregory A., Nurminen A., Kaguni LS., Mapping 136 Pathogenic Mutations into Functional Modules in Human DNA Polymerase γ Establishes Predictive Genotype-phenotype Correlations for the Complete Spectrum of POLG Syndromes. History of Health Science. 2014; (7): 1113–1121.

25. Lee Y., Kennedy WD, Yin YW., Structural Insight into Processive Human Mitochondrial DNA Synthesis and Disease-Related Polymerase Mutations. Cell 2009; 139, 312–324.

26. Graziewicz M.A., Longley M J., Copeland WC., DNA Polymerase γ in Mitochondrial DNA Replication and Repair. Chemical Reviews. 2006; 106, 383−405

27. Lodi T , Dallabona C. , Nolli C., Goffrini P., Donnini C., Baruffini E., DNA polymerase γ and disease: what we have learned from yeast. Frontiers in Genetics. 2015.

28. Gustafsson C. M., Falkenberg M., Larsson N., Maintenance and Expression of Mammalian Mitochondrial DNA. Annual Reviews. 2016; 85:9.1–9.28.

29. Sykora P, Kanno S Akbari M, Kulikowicz T, Baptiste BA, Leandro GS, Lu H, Tian J, May A, Becker KA, Croteau DL, Wilson DM III, Sobol RW , Yasui A, Bohr VA, DNA polymerase beta participates in mitochondrial DNA repair. Molecular and Cellular Biology. 2017.

30. Kazak L, Reyes A, Holt IJ., Minimizing the damage: repair pathways keep mitochondrial DNA intact. Nature Reviews. 2012; (13): 659–671.

31. Gredilla R, Bohr VA., Stevnsner T., Mitochondrial DNA repair and association with aging - an update. National Institute of Health 2010; 45(7-8): 478–488.

32. Gredilla R., Christian Garm C., Tinna Stevnsner T., Nuclear and Mitochondrial DNA Repair in Selected Eukaryotic Aging Model Systems. Oxidative Medicine and Cellular Longevity. 2012.

33. Copeland WC., The Mitochondrial DNA Polymerase in Health and Disease. National Institute of Health PA. 2010; 50: 211–222.

34. Fulda S., Galluzzi L., Kroemer G., Targeting mitochondria for cancer therapy, Nature Reviews. 2010.

35. Liberti MV, Locasale JW., The Warburg Effect: How Does it Benefit Cancer Cells?. HHS, 2016; 41(3): 211–218.

36. Dong L, Neuzil J., Mitochondria in Cancer: Why Mitochondria Are a Good Target for Cancer Therapy?. Elsevier. 2014; 127; 211-227.

37. Carlson EA., Yan SS., Disrupting cancer cell function by targeting mitochondria. Integrative Cancer Science and Therapeutics. 2014; 1(2): 17-25.

38. Orrenius S., Packer L., Cadenas E., Mitochondrial Signaling in Health and Disease. CRC Press. 2012; 60.

39. Sasaki R., Suzuki Y, Yonezawa Y., Ota Y, Okamoto Y., Demizu Y., Huang P., Yoshida H., Sugimura K, Mizushina Y., DNA polymerase γ inhibition by vitamin K3 induces mitochondria-mediated cytotoxicity in human cancer cells. Cancer Science. 2008. 99:1040-1048.

40. Guo G, Zhang F., Gao R., Delsite R., Feng Z., Powell SN., DNA repair and synthetic lethality. 2011; 3: 176-179.

41. O'Neil NJ., Bailey ML, Hieter P., Synthetic lethality and cancer. Nature Reviews. 2017.

42. Bridge G., Rashid S., Martin SA., DNA Mismatch Repair and Oxidative DNA Damage: Implications for Cancer Biology and Treatment. Cancers. 2014.

43. Martin S. A., McCabe N., Mullarkey M., Cummins R., Burgess DJ, Nakabeppu Y., Oka S., Kay E., Lord CJ., Ashworth A., DNA Polymerases as Potential Therapeutic Targets for Cancers Deficient in the DNA Mismatch Repair Proteins MSH2 or MLH1. Cell Press. 2017; 235–248, 2010.

44. Kim J., Genome editing comes of age. Nature. 2016.

45. Maeder M. L., Gersbach C. A., Genome-editing Technologies for Gene and Cell Therapy. Journal of the American Society of Gene & Cell Therapy. 2016; 24 (3), 430–446.

46. Ran F. A., Hsu PD., Wright J., Agarwala V., Scott DA, Zhang F., Genome engineering using the CRISPR-Cas9 system. HHS. 2013.

47. Nemudryi AA, Valetdinova KR., Medvedev SP., Zakian S. M., T ALEN and CRISPR/Cas Genome Editing Systems: Tools of Discovery. Acta Naturae. 2014; 22:19-40

48. Carroll D., Genome Engineering With Zinc-Finger Nucleases. Genetics. 2011; 188:

773–782.

49. Gaj T., Gersbach C. A., Barbas III C. F., ZFN, TALEN and CRISPR/Cas-based methods for genome engineering. NIH PA. 2013; 31(7): 397–405.

50. Yin H., Kauffman K. J, Anderson D. G., Delivery technologies for genome editing. Nature Reviews. 2017.

51. Shen S., Loh TJ., Shen H., Zheng X., Shen H., CRISPR as a strong gene editing tool. BMB Reports. 2017; 50(1): 20-24.

52. Torres-Ruiz R., Rodriguez-Perales S., CRISPR-Cas9: A Revolutionary Tool for Cancer Modelling. International Journal of Molecular Sciences. 2015; 16, 22151-22168.

53. Richter C., Chang JT., Fineran P. C., Function and Regulation of Clustered Regularly Interspaced Short Palindromic Repeats (CRISPR) / CRISPR Associated (Cas) Systems. Viruses. 2013; 4, 2291-2311.

54. Chen S., Sun H., Miao K., Deng C., CRISPR-Cas9: from Genome Editing to Cancer Research. International Journal of Biological Sciences. 2016; 12(12): 1427-1436.

55. Ran F. A., Hsu PD., Wright J., Agarwala C., Scott DA., Zhang F., Genome engineering using the CRISPR-Cas9 system. Nature Protocols. 2013; 8(11)2281-2308.

56. CRISPR Guide [Online] https://www.addgene.org/crispr/guide/

57. Kukat A., Kukat C., Brocher J., Scha¨fer I., Krohne G., Trounce IA., Villani G., Seibel P., Generation of ρ^0 cells utilizing a mitochondrially targeted restriction endonuclease and comparative analyses. Nucleic Acid Research. 2008.

58. Chevallet M., Lescuyer P., Diemer H., Dorsselaer A., Leize-Wagner E., Rabilloud T., Alterations of the mitochondrial proteome caused by the absence of mitochondrial DNA: A proteomic view. 2005. Electrophoresis. (27)1574–1583.

CURRICULUM VITAE

Personal Information

Name	Ayşegül	**Surname**	Ekmekçioğlu
Place of Birth	Şişli, İstanbul	**Date of Birth**	22.02.1993
Nationality	TC	**Telephone number**	05355123222
E-mail	aysegul.ekm@gmail.com		

Education

Level	**Institution Name**	**Graduation Year**
Master of Science	Acıbadem Mehmet Ali Aydınlar University	2018
Undergraduate	Yeditepe University	2016
High School	FMV Ayazağa Işık High School	2012

Work Experience

Position	**Corporation**	**Duration**
Research Assistant	Acıbadem Mehmet Ali Aydınlar University, Faculty of Arts and Sciences, Department of Molecular Biology and Genetics	08.2016-
Laboratory Intern	Istanbul University, Faculty of Medicine, Department of Medical Biology	07.2015-08.2015

Foreign Languages

Language	**Reading***	**Speaking***	**Writing***
English	Advanced	Good	Advanced
German	Intermediate	Beginner	Intermediate

***** Evaluated as advanced, good, intermediate, beginner

Foreign Language Exam Results [#]

YDS	YÖK-DİL	IELTS	TOEFL IBT	TOEFL PBT	TOEFL CBT	FCE	CAE	CPE

[#] All successful exams should be enrolled.

[#] YDS: Yabancı Dil Sınavı; YÖK-Dil: Yükseköğretim Kurumları Yabancı Dil Sınavı; IELTS: International English Language Testing System; TOEFL IBT: Test of English as a Foreign Language-Internet-Based Test TOEFL PBT: Test of English as a Foreign Language-Paper-Based Test; TOEFL CBT: Test of English as a Foreign Language-Computer-Based Test; FCE: First Certificate in English; CAE: Certificate in Advanced English; CPE: Certificate of Proficiency in English

Other Exams

Name of the Exam	**Quantitative**	**Equally Weighted**	**Verbal**
ALES**	63,49335	59,49632	54,29461

****** ALES: Akademik Personel ve Lisansüstü Eğitimi Giriş Sınavı

Computer Skills

Program	**Ability to Use**
Microsoft Office	Advanced
MATLAB	Beginner
R Studio	Beginner
CLC Mainworkbench 8.0	Intermediate

***** Evaluated as advanced, good, intermediate, beginner

Projects

Name of the Project	Institution	Position	Years
Development of the original 2-indolinone compounds as anti-interleukin 1 and chemotherapeutic drugs Sub-project 2: DNA repair inhibitors to be developed as a new drug for the treatment of hereditary nonpolyposis colorectal cancer (MLH1 gene defect). TUBITAK 1003, Project No: 215S614	Acıbadem Mehmet Ali Aydınlar University	Research Scholar	11.2016-07.2018
Determination of Small Molecule Inhibitors Blocking Mitochondrial Base Repairing Mechanism and Their Activities by Targeting DNA Polymerase Gamma Enzyme for Cancer Therapy. TUBITAK 1001, Project No: 212T026	Acıbadem Mehmet Ali Aydınlar University	Research Scholar	08.2016-11.2016
Senior Design Graduation Project: Observation of auto-fluorescence of cells treated with silver and gold nanoparticles	Yeditepe University	Researcher	2015-2016

Scholarships

Type	Institution	Years
MSc. Program of Medical Biotechnology, 100% Scholarship	Acıbadem Mehmet Ali Aydınlar University	2016-2018
100% Achievements Scholarship	FMV Ayazağa Işık High School	2007-2008

Conferences

Name of Conference	Position	Institution/Place	Duration/Year
Genome Maintenance, DNA Repair and Cancer	Organization committee and participant	Acıbadem Mehmet Ali Aydınlar University	26-28.04.2018
Thermo Fisher Scientific Day	Participant	Point Hotel	07.11.2018
EMBO Young Scientists' Forum	Participant	Boğaziçi University	05-06.01.2018
11th Aykut Kence Evolution Conference	Participant	Middle East Technical University	2017
5th Genetics and Bioengineering Days	Participant	Yeditepe University	2017
4th Genetics and Bioengineering Days	Participant	Yeditepe University	2016
11th Bioengineering Days	Participant	Ege University	2014
Destination and Imagination Activity	Participant	Robert College	2010

International and National Courses and Certificates

Name of Certificate	Institution	Year
Certificate of Experimental Animal Use	Acıbadem Mehmet Ali Aydınlar University, DEHAM	2016

Publications

Name of the Publication	Publisher	Year
Passion for German	Hürriyet DN GenNext	2010